Title	Minimizing Non-Specific Adsorption of Recombinant Adeno-Associated Virus Vectors on Solid Surfaces through the Application of a Polyionic Hydrophilic Complex (AP1) Coating
Author(s)	Salama, Ramy Essameldine Abdelhady
Citation	大阪大学, 2024, 博士論文
Version Type	VoR
URL	https://doi.org/10.18910/98644
rights	
Note	

Doctoral Dissertation

Minimizing Non-Specific Adsorption of Recombinant Adeno-Associated

Virus Vectors on Solid Surfaces through the Application of a Polyionic

Hydrophilic Complex (AP1) Coating

RAMY ESSAMELDINE ABDELHADY SALAMA

May 2024

Macromolecular Biotechnology Laboratory

Department of Biotechnology

Division of Advanced Sciences and Biotechnology

Graduate School of Engineering

Osaka University

Contents

List of Abbreviations

(in alphabetical order)

AAP: assembly-activating protein.

AAV: adeno-associated virus.

COP: cyclic olefin polymer.

ddPCR: digital droplet PCR.

D-PBS (−): Dulbecco's phosphate-buffered saline without calcium and magnesium.

EMA: European Medicines Agency.

F/T cycles: freeze/thaw cycles.

FDA: US Food and Drug Administration.

GFP: green fluorescent protein.

IEE: Integration Efficiency Element.

ITRs: inverted terminal repeats.

kb: kilobases.

P188: Poloxamer 188.

PBS: phosphate-buffered saline

PHC: polyionic hydrophilic complex.

pI: isoelectric point.

PMDA: Pharmaceuticals and Medical Devices Agency.

PS20: Polysorbate 20.

PS80: Polysorbate 80.

qPCR: quantitative polymerase chain reaction.

rAAV: recombinant adeno-associated virus.

RSS: reference standard stock.

SMA: Spinal Muscular Atrophy.

VG: vector genome.

VP: viral capsid protein.

YFP: yellow fluorescent protein

Chapter 1

General Introduction

1.1. Gene therapy concept

Gene therapy, a kind of molecular medicine, holds considerable promise for impacting human health in the current era. It offers the potential for novel treatments for numerous inherited and acquired diseases. The fundamental concept of gene therapy is simply introducing a segment of genetic material into specific cells to either cure or decelerate the progression of a disease.[1] Gene therapy offers undeniable therapeutic benefits compared to current treatment methods like small molecules or biologics. These advantages encompass correcting the genetic root of a disease, precisely targeting affected cells and tissues for treatment, allowing these cells and tissues to produce their own therapeutic agents, and providing long-lasting treatment effects after a single administration.[2]

1.2. Gene therapy perspectives

The identification of DNA as the biomolecule governing genetic inheritance and disease has catalyzed the exploration of therapeutic avenues, wherein aberrant genes may be modified to enhance human well-being. The recent capacity for expeditious and cost-effective human genetic analyses on extensive populations, coupled with the sequencing of complete genomes, has created a proliferation of nucleic acid sequence data. This wealth of information facilitates the elucidation of the specific gene or genes underpinning a given pathological state. If rectification of mutated genes or normalization of the expression of hyperactive/hypoactive genes is achievable, diseases may be addressed at the molecular level, with the potential for cure in optimal scenarios. This paradigm holds

particular applicability in the context of monogenic diseases, characterized by mutations in a singular gene. This ostensibly straightforward premise has been the focal point of gene therapy endeavors for over four decades.[3]

1.3. The gene therapy vehicle

Nevertheless, achieving the delivery of essential nucleic acid cargoes into the intracellular environment posed a formidable challenge until the advent of utilizing viruses as delivery vehicles. This groundbreaking approach leverages the inherent ability of viruses to efficiently introduce their nucleic acids into host cells, thereby overcoming the historical obstacles associated with intracellular delivery. The strategic integration of viruses as carriers not only revolutionized the field of nucleic acid delivery but also led to a new era of possibilities for targeted and efficient transport within cellular frameworks. This transformative use of viruses in the delivery process has significantly expanded our capacity to manipulate cellular genetic material, paving the way for advancements in various biomedical applications and therapeutic interventions.[3] Due to the growing interest in gene therapy, scientists use different viral vectors, each with its own unique qualities. These vectors help researchers customize their methods based on specific needs. These viral vectors have different strengths, like how well they can deliver genes, how much they can carry, and how safe they are. Examples include retroviruses, lentiviruses, adenoviruses, and adeno-associated viruses.[4] Knowing the strengths and limitations of each helps scientists choose the right tool for the job. This variety highlights the evolving nature of gene therapy and emphasizes the importance of understanding these tools to use them effectively for targeted and successful treatments.[4]

1.4. Utilizing viruses as a gene therapy vector

A virus is a biological entity capable of infiltrating the host cell nucleus, leveraging the cellular machinery to transcribe and replicate its genetic material, facilitating subsequent dissemination to neighboring cells.[5] Researchers employ diverse viral vectors to introduce therapeutic genes into cell nuclei, capitalizing on the inherent biological processes of the virus life cycle. Utilizing a virus as a gene transfer vector necessitates genetic engineering modifications. Specifically, the pathogenic elements within its genetic makeup are excised and substituted with the therapeutic gene payload.[6] Simultaneously, the virus keeps its non-harmful components, such as envelope proteins and capsid proteins. These elements enable the virus to enter and infect the cell.[5] The resultant non-pathogenic virus, bearing the therapeutic gene, is denoted as a viral vector. Presently, viral vectors predominate as the preferred gene transfer vehicles, owing to their notable efficiency in in vivo gene transfection.[7]

1.5. Viruses commonly used as gene therapy vectors

Most viral vectors used nowadays are adenoviruses, adeno-associated viruses (AAV), retroviruses, lentivirus and simple herpes virus.[8]

Table 1.1. outlines the main viruses employed as gene transfer systems, providing concise descriptions of the strengths and limitations associated with each virus.[9] [10]

Vector	strengths	limitations
Adenovirus	- Very high titers (10^{12} pfu/mL). - High transduction efficiency ex vivo and in vivo.	- Remains episomal. - Transient expression. - Requires packaging cell line.

	• Transduces many cell types. • Transduces proliferating and nonproliferating cells. • Production easy at high titers.	• Immune-related toxicity with repeated administration. • Potential replication competence. • No targeting. • Limited insert size: 4–5 kb.
Adeno-associated virus	• Integration on human chromosome 19 (wild type only) to establish latent infection. • Prolonged expression. • Transduction does not require cell division. • Small genome, no viral genes.	• Not well characterized No targeting. • Requires packaging cell line. • Potential insertional mutagenesis. • High titers (10^{10} pfu/mL) but production difficult. • Limited insert size: 5 kb.
Herpes simplex virus	• Large insert size: 40–50 kb. • Neuronal tropism. • Latency expression. • Efficient transduction in vivo. • Replicative vectors available.	• Cytotoxic. • No targeting. • Requires packaging cell line. • Transient expression does not integrate into genome. • Moderate titers (10^4–10^8 pfu/mL).
Lentivirus	• Transduces proliferating and nonproliferating cells. • Transduces hematopoietic stem cells.	• Safety concerns: from human immunodeficiency virus origin. • Difficult to manufacture and store.

	• Prolonged expression. • Relatively high titers (10^6–10^7 pfu/mL).	• Limited insert size: 8 kb. • Clinical experience limited.
Retrovirus	• Integration into cellular genome. • Broad cell tropism. • Prolonged stable expression. • Requires cell division for transduction. • Relatively high titers (10^6–10^7 pfu/mL). • Larger insert size: 9–12 kb.	• Inefficient transduction. • Insertional mutagenesis. • Requires cell division for transfection. • Requires packaging cell line. • No targeting. • Potential replication competence.

1.6. Adeno-associated virus as a gene therapy vector

Adeno-associated virus (AAV) has emerged as a prominent subject of investigation in gene therapy. Its initial discovery occurred as an incidental finding during the handling of adenovirus preparations.[11] [12] Consequently, as implied by its name. To put it in simpler terms, AAV has a protective protein shell safeguarding a small, single-stranded DNA genome, approximately 4.8 kilobases (kb) in size. AAV belongs to the parvovirus family and relies on co-infection with other viruses, primarily adenoviruses, for replication. Initially differentiated through serological means, molecular cloning has revealed numerous unique AAV strains across species. Its genome, consisting of three genes (Rep, Cap, and aap), yields at least nine gene products through distinct promoters, alternative translation start sites, and differential splicing. These coding sequences are bordered by inverted terminal repeats (ITRs), crucial for genome replication and packaging. The Rep

gene produces four proteins (Rep78, Rep68, Rep52, and Rep40), essential for viral genome replication and packaging. Simultaneously, Cap expression results in viral capsid proteins (VP; VP1/VP2/VP3), forming the outer protective shell and actively participating in cellular binding and internalization. The viral coat is thought to consist of 60 proteins organized into an icosahedral structure, with the capsid proteins in a ratio of 5:5:50 (VP1:VP2:VP3)[13], whereas recent studies have clarified the ratio is not exact 5:5:50 ratio but varies by unidentified mechanism.[14] The aap gene produces the assembly-activating protein (AAP) in a different reading frame that overlaps with the cap gene. This nuclear protein is believed to play a role in providing structural support for capsid assembly.[15] AAP plays a crucial role in localizing VP proteins to the nucleolus and facilitating capsid assembly in AAV2. However, in 11 other recently studied serotypes, the subnuclear localization of AAP varies. Additionally, AAP is not essential in AAV4, AAV5, and AAV11.[16] Various factors need to be taken into account when using a viral vector. These factors encompass the capacity to bind to and enter the target cell, efficient transfer to the nucleus, sustained expression within the nucleus, and a minimal level of toxicity. AAV vectors have proven notably successful in meeting all these requirements. Furthermore, numerous modifications have been implemented to augment their effectiveness. The development of current AAV vectors has been influenced by specific considerations, particularly the non-pathogenic nature of the wild-type virus and its enduring presence.[17] Due to the AAV genome's small size and worries about Rep influencing cellular gene expression, researchers created AAV vectors without Rep and the integration efficiency element (IEE), crucial for frequent site-specific integration. Recombinant adeno-associated virus (rAAV) which lacks viral DNA, is essentially a

protein-based nanoparticle designed to penetrate the cell membrane, enabling the delivery of its DNA cargo into the cell nucleus. In the absence of Rep proteins, the transgenes flanked by ITRs within rAAV can combine to form circular concatemers, persisting as episomes within the nucleus of transduced cells.[18] Although the ITRs are retained as essential signals for packaging, current rAAV vectors mainly exist as extrachromosomal elements, avoiding integration into the host's chromosomes.[19] Since recombinant episomal DNA doesn't integrate into host genomes, it gradually diminishes as cells replicate. Consequently, transgene and transgene expression loss occur over time, with the rate of loss determined by the turnover rate of transduced cells. These attributes render rAAV particularly suitable for specific gene therapy purposes.[20]
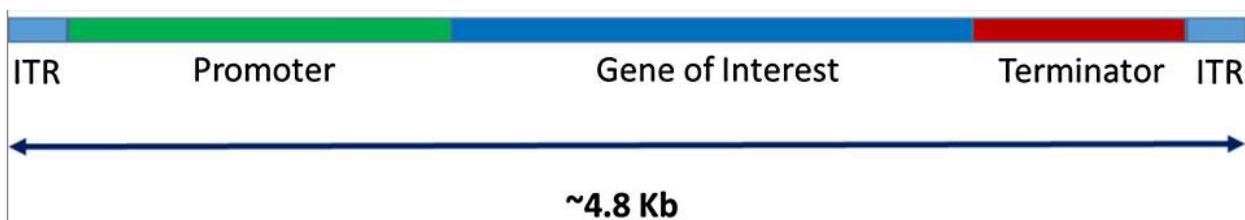
Figure 1.1. Schematic representation of the basic components of a gene insert packaged inside recombinant AAV gene transfer vector. AAV adeno-associated virus, ITR inverted terminal repeat.[20]

1.7. rAAV advantages and disadvantages

rAAV carrier vectors have proven successful due to their numerous advantages. rAAVs are non-pathogenic gene therapy vectors lacking the ability to replicate. They have been utilized in clinical settings since 1995. Upon administration, they exhibit efficient transduction, leading to stable and prolonged transgene expression, particularly in non-dividing cells.[21] Numerous AAV serotypes exist, comprising 12 natural variants and over 100 synthetic variants. These distinct serotypes have varying abilities to transduce

different tissues.[22] [23] Choosing the right AAV serotype is crucial when creating gene therapy based on rAAV. Different serotypes have affinities for specific tissues, and understanding how the dose of the AAV affects its distribution to tissues is important for evaluating safety and effectiveness. Improving the therapy's efficacy and selectivity can be achieved by using a different AAV serotype, changing the capsid through techniques like site-directed mutagenesis, or modifying elements of the expression cassette, such as the enhancer or promoter, or the size, activity, or codon of the transgene. However, there are also drawbacks to using rAAVs in gene therapies. For instance, AAVs have a limited capacity to carry genetic material, restricting the size of the transgene used in gene therapy to less than 4.8 kb. Additionally, during cell division, the episomal DNA of the rAAV-based gene therapy may be spread out among daughter cells, potentially reducing efficacy in rapidly growing organs, such as the liver in neonates.[24] Moreover, rAAV could result in immunological responses in patients treated with rAAV drug product. rAAV vectors are relatively uncomplicated in terms of their immunogenicity since they lack viral proteins and consist of a protein shell enclosing a DNA genome. Nevertheless, previous exposure to wild-type AAV can trigger both antibody and cellular immune responses against the virus, potentially affecting AAV vector efficacy. Existing antibody responses (neutralizing antibodies) pose a notable obstacle to achieving successful gene transfer through systemic administration of AAV vectors.[25]

1.8. In market

Since the initial clinical investigation employing rAAV for cystic fibrosis in the 1990s[26], significant advancements have been achieved in comprehending its virology, production, safety, efficacy, and translational potential.[27] In the last decade, rAAV has been widely

used in treating rare diseases affecting brain, heart, liver, muscle, eye, and other tissues.[28] Prolonged expression of the transgene has been accomplished in numerous trials, resulting in extensively investigation in clinical trials for many diseases, including hemophilia B,[29] Leber congenital amaurosis,[30] and lipoprotein lipase deficiency[31] besides, a bunch of therapies securing approval from both the US Food and Drug Administration (FDA) and the Japanese Pharmaceuticals and Medical Devices Agency (PMDA) (Luxturna, Zolgensma) as well as the European Medicines Agency (EMA) (Glybera, Luxturna, Zolgensma, Upstaza, Roctavian).[32] [33]

1.9. Cost

Despite these extraordinary achievements in using rAAV, one of the most significant challenges for AAV-based gene therapy is the cost of the drug product. For instance, alipogene tiparvovec (Glybera), priced at 1 million euros (US$1.2 million) per patient recorded as the world's most expensive drug prior to its withdrawal from the market in 2017 due to insufficient demand;[34] voretigene neparvovec-rzyl (Luxturna), introduced in 2017 at US$425,000 per eye treatment, also comes with a high price; onasemnogene abeparvovec-xioi (Zolgensma) that costs $2.125 million.[35] and finally, etranacogene dezaparvovec-drlb (Hemgenix) currently holds the title of the world's most expensive drug, with a cost of $3.5 million.[36] Unfortunately, this cost is mainly due to the expensive manufacturing process.[27] Generating sufficient vector quantities for the targeted treatment of specific organs, such as the CNS, liver, or muscles, as well as achieving multi-organ targeting across the body, necessitates substantial resources and expertise within current production systems. This includes aspects like production, quality control, and assay standardization.[27] Additionally, there are significant costs associated with

preclinical studies, encompassing toxicity, safety, dosing, and biodistribution assessments, typically mandated for approval by FDA.[37] Furthermore, the analytical and scientific research methods essential for studying rAAVs demand specialized instruments and expensive tools and reagents. This poses a barrier for some laboratories, preventing them from either producing rAAVs or acquiring purified vectors in small-scale preparations.[38] Consequently, there is a pressing need for more cost-effective methods in the production and analysis of rAAV vectors that can maintain both a high yield and quality.[39]

1.10. Challenges facing manufacturing of rAAV

The production of AAV viral vectors is a complex endeavor, requiring innovative approaches to ensure they meet safety and efficacy standards, as well as clinical and market demands, while staying within cost targets. Maintaining the stability of viral vectors, preventing degradation during manufacturing, handling, and storage, and ensuring their long-term efficacy are significant challenges for AAV manufacturers. To overcome these challenges, a combination of traditional methods and new technologies is necessary to develop scalable and robust manufacturing processes for gene therapy products.[40] The process of manufacturing viral vectors faces various challenges during the upstream and downstream operations, as well as formulation and fill/finish processing steps.[40] Challenges in upstream processing include, plasmid development, cell expansion and plasmid transfection. While challenges in downstream processing step include cell lysis, filtration, purification and separation of empty capsids from full capsids. Finally, the key challenges in formulation and the unit operations of fill/finish lie in identifying optimal solution conditions for different routes of administering gene therapy products (e.g.,

14

intravenous, subcutaneous, intrathecal, subretinal), and in minimizing product degradation during manufacturing, aseptic fill/finish procedures, and storage.[40]

When it comes to product degradation, viral vectors face several hurdles throughout manufacturing, storage, shipping, and handling, potentially affecting the safety and effectiveness of AAV products. The degradation of AAV can be categorized into physical and chemical instabilities. The breakdown of viral vectors is influenced by solution conditions, notably pH, ionic strength, and impurities from raw materials or additives, as well as external factors like temperature, shear stress, freeze/thaw cycles, and light exposure.[41] [42] Degradation Mechanisms of AAV vector include physical Instability, denaturation/unfolding, aggregation, surface adsorption, chemical instability, disulfide formation/exchange, deamidation, oxidation and isomerization.[40]

In this study I focused on the viral vectors surface adsorption that is one of the main challenges facing the formulation and fill/finish processing steps as well as analysis and quality control steps. During manufacturing and until analytical steps of quality control or research, viral vectors may adhere to surfaces such as tubing, glass, plastic, and stainless steel, as well as the drug product container and closure, causing surface-induced aggregation. This leads to the accumulation and binding of protein molecules onto these surfaces, resulting in physical degradation and alterations in the conformation and state of the protein molecules.[43] [44] The capsid proteins of viral vectors, like other protein therapeutics, have the propensity to adhere to a range of surfaces when subjected to interfacial stresses. This adherence can trigger protein unfolding, aggregation, and precipitation, consequently diminishing the concentration of AAV in solution.[45] [46] Misfolded capsid proteins could expose hydrophobic residues, promoting protein

15

aggregation through hydrophobic interactions. This process can give rise to initial small aggregates, which can serve as seeds for further AAV aggregation, ultimately leading to the emergence of visible particles within the solution.[40]

1.11. Surface adsorption of viral particles
The adsorption of most viruses can be classified into two stages:

(1) Specific adsorption that is characterized by the precise recognition and binding of viral surface proteins (antigens) to their corresponding receptors on the host cell membrane. This binding event triggers subsequent signals, setting off the internalization process of the viruses.[47] [48]

(2) Non-specific adsorption that occurs when viruses come into contact-randomly- with a surface (cellular or non-cellular) through intra-molecular forces, hydrophobicity, ionic, and electrostatic interactions. [49] [40]

The rAAV non-specific adsorption onto solid surfaces stands out as a primary factor contributing to vector loss during storage and transfer, as well as a cause for diminished vector genome (VG) quantification values. Especially that the typical concentration ranges of rAAV vector particles are generally characterized by relatively low protein concentrations.[50] Non-specific adsorption of AAV particles onto surfaces may occur during manufacturing depending on the process and solution conditions.[40] It may also occur during product delivery through an administrative device.[51] The exploration of viral vectors' non-specific adsorption has been a subject of previous investigations. These studies mentioned that these vectors, in various stages of manufacturing, analysis, and storage, exhibit a tendency to adhere indiscriminately to surfaces composed of glass, plastics, and stainless steel.[40] [52] The adherence of vector particles to surfaces can

16

exhibit notable differences, even among materials with similar compositions, leading to varying degrees of particle loss.[53] Earlier investigations exploring the incubation of rAAV with commonly encountered laboratory materials, including stainless steel, polypropylene and nitinol revealed a substantial time-dependent loss of vector particles, with reports indicating up to a 50% reduction in the original rAAV count due to adsorption.[54] [55] During a preclinical investigation, it was observed that AAV5 vector particles experienced notable loss as a result of their adsorption onto glass and plastic surfaces, underscoring the importance of considering surface interactions in experimental settings.[56] In a recent investigation, the preservation of AAV in containers made of glass was examined, specifically in a direct comparison with containers made of cyclic olefin polymer (COP). The findings revealed a significantly greater AAV recovery following storage in COP containers compared to storage in glass containers. This outcome highlights the heightened propensity of AAV vectors to adhere to glass surfaces compared to COP surfaces.[57] Other research has indicated that AAV adsorption is higher on glass and polypropylene compared to polystyrene.[58] Examinations into the stability of rAAV2 Reference Standard Material disclosed that storing it in both glass-made and polypropylene-made containers led to a noteworthy decrease in the vector titer, ranging between 30% and 40%.[59] Additional studies have revealed that vector loss, at times ranging from 75% to 90%, is attributable to nonspecific binding on the surfaces of tools used in preparing dilutions. Moreover, adsorption onto the inner walls of loading syringes and surfaces of surgical delivery equipment, such as polypropylene, Teflon, stainless steel, polycarbonates and fused silica, is observed unless a surfactant is incorporated into the vector formulation.[51] [60] [61] [62] [63] Accordingly, non-specific adsorption of

rAAV is a serious issue specially when considering cost and dosing or the amount of vector that should be given to patients especially that these doses are usually of a high amount of the rAAV vector. As an illustration, doses administered in certain clinical trials were documented to be 10^4-fold greater than that of Luxturna (at a dose of 1.5×10^{11}/eye).[64] This poses not only a manufacturing challenge but also raises safety concerns. For instance, in the ASPIRO phase-2 trial (NCT03199469) targeting X-linked myotubular myopathy, the administration of a dose equivalent to 3×10^{14} rAAV8 viral genomes (vg)/kg resulted in two patient deaths attributed to sepsis.[64] When rAAV particles unintentionally adhere to surfaces, during manufacturing, analysis, or storage, it can lead to significant loss of the viral vector. This not only decreases the efficiency of the gene therapy but also raises concerns about consistent and predictable dosing. These circumstances show why the challenge of non-specific adsorption of rAAV represents a critical issue in gene therapy. Solving the issue of non-specific adsorption is imperative to ensure the reliability and effectiveness of gene therapies utilizing rAAV vectors.[65]

1.12. Surfactants as a solution for adsorption issue.

As a result of the emerging non-specific adsorption of rAAV, many studies have investigated surfactants to control the issue of the proteins on encountered surfaces, and indeed surfactants played a crucial role in eliminating the adsorption of proteins on surfaces. Surfactants exert their action by impeding the adsorption of proteins to interfaces, acting as a physical barrier to prevent the establishment of a protein layer at the interface. The heightened surface activity of surfactants results in an increased effective concentration of these additives at interfaces relative to the bulk solution. Hence, the wise addition of an appropriate quantity of surfactant, typically sufficient to saturate

the interface, proves efficacious in frustrating undesired protein adsorption and mitigating aggregation throughout the processes of storage, filtration, purification, filling, and transportation.[65]

Poloxamers, often denoted by the abbreviation "P" followed by three digits, are artificial tri-block copolymers. They consist of a central hydrophobic chain made of polyoxypropylene flanked by two hydrophilic chains of polyoxyethylene, with a weight ratio of 4:2:4. This molecular arrangement creates an amphiphilic surface copolymer.[66] Within the Poloxamer family, Poloxamer 188 (P188) stands out as a biocompatible and non-ionic linear copolymer. This molecule comprises two sections: one block consists of 38 units of hydrophilic polyoxyethylene, sandwiching another block comprising 29 units of hydrophobic polyoxypropylene. Its molecular weight is 8400 Daltons.[67]

P188 is considered one of the extensively studied surfactants employed to reduce vector adsorption onto packaging materials, and it is frequently incorporated into rAAV products.[68] The FDA has granted approval for the utilization of P188 at varying concentrations, dependent on the chosen route of administration;[69] 0.001% P188 in phosphate-buffered saline (PBS) is commonly added into rAAV suspension formulations.[51] [70] [71] [72]

Polysorbates are amphipathic surfactants that lack ionic properties, consisting of fatty acid esters combined with polyoxyethylene sorbitan. Among them, Polysorbate 20 (polyoxyethylene sorbitan monolaurate) and Polysorbate 80 (polyoxyethylene sorbitan monooleate).[73] Polysorbate 80 (PS80) and Polysorbate 20 (PS20) are widely utilized surfactants in approved protein biologic drug products for injection, typically within a concentration range of 0.001% to 1% (w/v).[65] They are used also to minimize surface

adsorption of therapeutic proteins as well as decreasing aggregation and denaturation of the protein drug product.[74] Recently, PS20 has been used in the formulation of rAAV vector products such as (Hemgenix).[75]

1.13. Surfactants drawbacks

Indeed, formulations of rAAV are typically subjected to dilution prior to aliquoting for the purpose of sampling for transduction of cell lines,[76] sampling for VG quantification,[77] [78] and/or given to patients.[79] However, this process leads to a diluted surfactant concentration, diminishing the intended effect and increasing vector adsorption. Additionally, P188 is prone to oxidation unless supplemented with antioxidants.[80] [81] [82] A recent investigation explored the behavior of P188 under different storage conditions, revealing that its stability changes based on the buffer environment. The study suggests that P188 is susceptible to degradation, potentially shortening the shelf life of the drug product.[83] Polysorbates are also susceptible to degradation through two primary mechanisms: hydrolysis and oxidation pathways. These pathways represent distinct routes through which the chemical structure of polysorbates can break down, potentially impacting the integrity and effectiveness of the drug product.[84] Furthermore, reports indicated variations in the shelf-life of different AAV formulations, which encompassed distinct surfactants (such as P188 and PS20) and varying concentrations of protamine.[85] Hence, surfactants could potentially contribute to the instability of AAV; nevertheless, additional research is still needed.

1.14. Research objective

In this investigation, I explored the prevention of rAAV vector loss caused by adsorption by examining the potential of an alternative to the typically used surfactants. My goal was to enhance VG recovery and achieve more accurate quantification, ensuring the persistence of the adsorption prevention effect regardless of the dilution of the vector formulation and bypassing the issue of surfactants degradation. According to a study by Elwing *et al*., it has been found that protein adsorption generally rises on relatively hydrophobic surfaces. Particularly, the amount of negatively charged protein adsorbed tends to be higher on surfaces with a relatively large contact angle of water.[86] [87] In this current study, I employed a polyionic hydrophilic complex (PHC) polymer coating on the tools utilized in rAAV vector analyses—specifically, pipette tips, cryotube vials, and quantitative polymerase chain reaction (qPCR) plates. The chosen coating polymer is an ultra-thin film recognized for its biocompatibility and deemed safe for clinical use. It comprises phosphate moieties and amine groups that confer zwitterionic properties, in addition to being heat resistant up to 95 °C.[88]
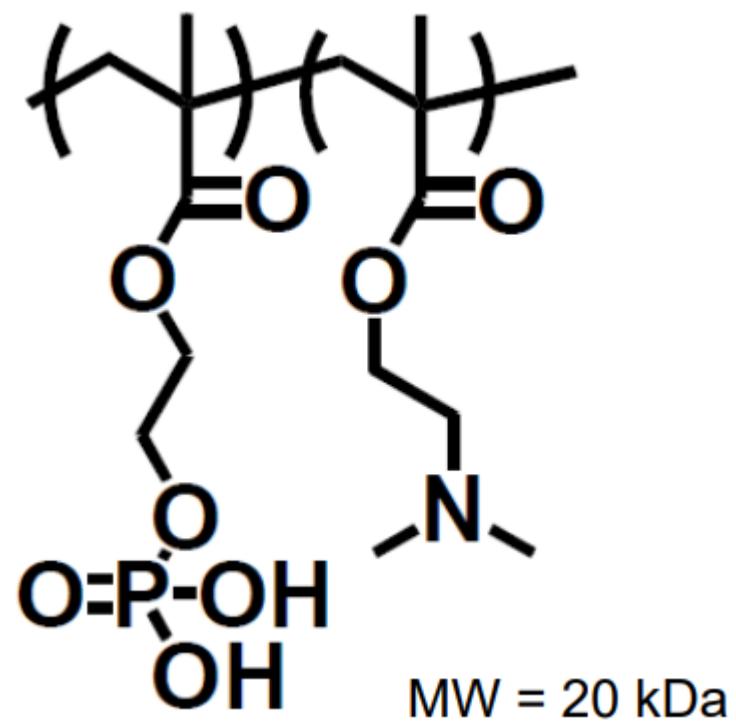
Figure 4.1. PHC coating chemical structure.[89]

Chapter 2

Investigating the applicability of the PHC coating in minimizing the non-specific adsorption of rAAV

2.1. Introduction

Quantification of rAAV VG is a crucial step in vector production, quality control, and even in analytical research aspects. A precise genome titer is essential not only for determining clinical dosages but also as a fundamental requirement for numerous analytical assays used in the characterization of AAV products.[90] For this purpose, qPCR has emerged as the predominant and widely embraced technique for AAV vector quantification due to its simplicity and robustness when operating under optimal conditions.[91] In this chapter, the focus was directed towards examining the PHC coating applied to tools commonly utilized during the analysis of rAAV. For analytical purposes, rAAV samples are typically stored and transported in cryotube vials. Quantification of rAAV VG through qPCR is performed using pipettes equipped with their respective tips, in addition to qPCR plates. All these tools are polypropylene made. And as mentioned in the previous chapter, rAAV vectors can adsorb on to plastic materials like polypropylene. Therefore, I coated these tools with the PHC coating to investigate its efficiency in decreasing rAAV adsorption. I primarily selected the rAAV1 serotype for investigation due to its extensive study and research within the field. Currently, rAAV1 is under investigation in numerous phase-2 clinical trials, including but not limited to studies focusing on Alpha-1 Antitrypsin Deficiency, Ischemic Cardiomyopathy, and Duchenne Muscular Dystrophy.[40] Additionally, rAAV2 and rAAV8

were employed to ascertain whether the impact of the PHC coating on reducing rAAV adsorption varies based on serotype. In addition, I have studied the alterations in the characteristics of solid surfaces subsequent to the application of PHC coating by measuring the contact angle and zeta potential for surfaces before and after being coated with PHC coating.

Contact angle measurement provides a qualitative assessment of a surface's hydrophobic or hydrophilic nature. This method relies on observing the interactions between the surface and a small water droplet when it makes contact. It is primarily employed to test surface wettability.[92] Contact angle measurement can be conducted using either the sessile drop method or the captive bubble method. In the sessile drop approach, a droplet, usually water, is deposited onto the solid sample, and its image is captured by a high-resolution camera. Software then automatically determines the contact angle. This method provides a static contact angle for the surface. Sessile drop measurements are typically carried out with water, where a contact angle below 90 degrees indicates hydrophilicity and above 90 degrees indicates hydrophobicity.[93] The disadvantage of this method is that the contact surface and probe liquid (water drop) are susceptible to dehydration during the measurement because the surface is exposed to air.[94]

In the captive bubble method, contact angles are measured with the sample submerged in a liquid, typically water. An air bubble or a less dense liquid, such as oil, is employed for measurements. The angle between the air bubble and the submerged surface is then measured in a similar manner to the sessile drop method.[93] However, dehydration of the sample is not a concern as it remains suspended in liquid.

Implementing the captive bubble technique typically requires more time compared to the sessile drop technique due to the time-consuming process of aligning the bubble with the surface being tested.[94]
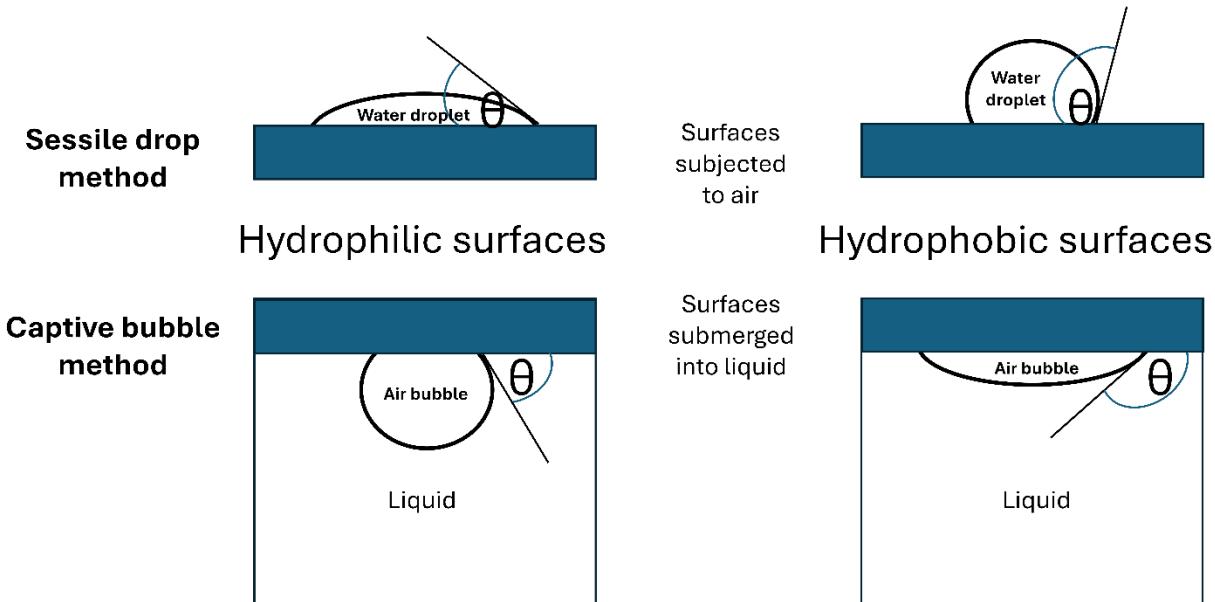
Figure 2.1.1. An illustrative diagram showing differences between the two used methods for measuring the contact angle (θ) of a surface. In the sessile drop method, a droplet of liquid is placed onto the surface whose contact angle is being measured. The droplet is typically formed using a syringe or a similar apparatus, and it naturally spreads out on the surface due to surface tension. The contact angle is then measured as the angle formed between the tangent to the droplet at the point where it meets the surface and the surface itself. This method is widely used and relatively straightforward, requiring minimal equipment. The material is considered hydrophilic if (θ) is lower than 90 degrees and hydrophobic if larger than 90 degrees. **In the captive bubble method**, a bubble of gas is introduced underneath the surface of a liquid that is in contact with the surface being studied. The bubble is typically introduced using a fine needle or similar device, and it adheres to the surface due to surface tension. The contact angle is determined by measuring the angle formed between the tangent to the bubble's interface at the point of contact with the solid surface and the solid surface itself, typically using optical techniques

such as image analysis. This method is particularly useful for surfaces that are not easily wetted by liquids, as it allows for the measurement of the contact angle without needing the liquid to spread out on the surface. On the other hand, the material is considered hydrophilic if (θ) is larger than 90 degrees and hydrophobic if lower than 90 degrees.[93]

The zeta potential, also referred to as electrokinetic potential, emerges at the interface between a material and a liquid medium. It's a characteristic property that's usually quantified in millivolts. When a material encounters a liquid, the functional groups on its surface interact with the surrounding medium, leading to the formation of a surface charge. This charge attracts oppositely charged ions, resulting in the formation of an electrochemical double layer. The zeta potential represents the combined effect of the initial surface charge and the accumulated layer of ions. Therefore, it represents the net charge of a surface that is in contact with a liquid. At its simplest, measuring zeta potential provides an answer to whether the electrical charge on the material particle is positive or negative.[95] [96] [94]
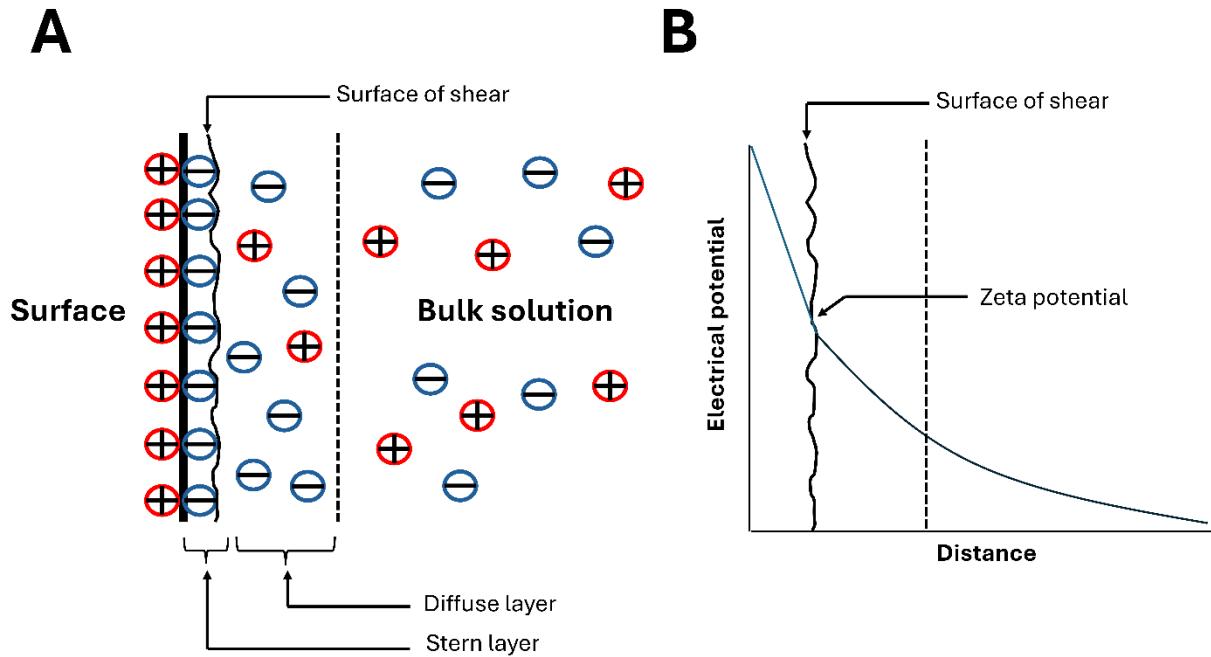
Figure 2.1.2. An illustrative diagram showing the concept and definition of the zeta potential measurement. Zeta potential denotes the electric charge formed at the boundary between a solid surface and its liquid environment, typically quantified in MilliVolts. Several mechanisms can contribute to this potential, including the dissociation of ionizable groups on the particle surface and the selective adsorption of solution ions onto the surface. The resultant charge on the particle surface influences the distribution of ions nearby, leading to an increased concentration of counterions near the surface and the formation of an electrical double layer at the particle-liquid interface. This double layer (**A**) comprises two segments: an inner section containing ions tightly bound to the surface and an outer section where the distribution of ions is determined by a balance between electrostatic forces and random thermal motion. Consequently, the potential in this outer region diminishes as the distance from the surface increases, eventually reaching the bulk solution value, typically assumed to be zero. This decline, illustrated in (**B**), highlights that the zeta potential represents the value at the surface under shear.[97]

2.2. Materials and methods

2.2.1. Coating tools with the PHC coating

Pipette tips with volume ranges 0.5–2, 2–200, and 50–1000 μL (Eppendorf, epT.I.P.S. Reloads, Hamburg, Germany), 1-mL cryotube vials (377224, Thermo Fisher Scientific, Waltham, MA, USA), and MicroAmp™ Fast Optical 96-Well Reaction Plates with Barcode, 0.1 mL (4346906, Thermo Fisher Scientific), all made of polypropylene, were employed in this study. These tools underwent coating with the PHC coating material (prevelex® AP1; Nissan Chemical Corporation, Tokyo, Japan). The experimental controls involved the use of tools in their initial, non-coated condition.

The coating solution was prepared by dissolving the polymer powder in to water/ethanol solvent and pH of the solution was adjusted to pH 3 using 1 mol/L HCl aq. The polymer is polymerized in a water/ethanol solvent at acidic pH and then diluted to prepare the coating solution.

The pipette tips' ends were enveloped with parafilm (PARAFILM M, P7793, Sigma-Aldrich), and the PHC coating solution was introduced from the top to exclusively coat the interior of the tips. Subsequently, the solution was extracted, and the tips were allowed to dry for 3 hours at 25 °C. This was followed by three washes with ultrapure water and another drying period of 3 hours at 25 °C.

For coating the cryotube vials and the 96-well qPCR plates, the coating solution was introduced into the vials or wells of the plates. Subsequently, the solution was withdrawn, and the vials or plates were left to dry for 3 hours at 25 °C. This was followed by three washes with ultrapure water and an additional drying period of 3 hours at 25 °C.

2.2.2. Quantitative analysis of rAAV VG using qPCR with PHC-coated and non-coated tools

The Manufacturing Technology Association of Biologics, Tokyo, Japan, supplied surfactant-free rAAV1 vector suspension stocks expressing the ZsGreen1 green fluorescent protein (GFP) reporter gene under the control of a cytomegalovirus promoter, flanked by AAV type 2 inverted terminal repeats. These vector stocks were formulated in 1× PBS at pH 7.4 (10010023, Thermo Fisher Scientific) with nominal concentrations of 2.29×10^{12} VG/mL and 5.82×10^{12} VG/mL. rAAV1 (9.8×10^{12} VG/mL), rAAV2 (6.5×10^{12} VG/mL), and rAAV8 (1.8×10^{13} VG/mL) suspension stocks formulated in PBS that contains surfactant (0.001% P188) were purchased from Addgene (105545-AAV1, 105545-AAV2, and 105545-AAV8, respectively; Watertown, MA, USA). All the aforementioned vector stocks were diluted by a factor of 100 using (1×) PBS at pH 7.4. (10010023, Thermo Fisher Scientific) in cryotube vials just prior to the qPCR analysis. Pipetting was employed for the handling, dilution, sampling, transfer, and distribution of these vector suspensions. Subsequently, sample preparation and qPCR analysis adhered to the AAV titration kit protocol (6233, AAVpro Titration Kit for Real-Time PCR Ver.2, Takara Bio, Kusatsu, Shiga, Japan). Notably, qPCR plates were utilized in the sample preparation stage, instead of using separate tubes, to minimize potential variability that could arise during the preparation steps. The preparation required incubation at different temperatures, which was achieved using two thermocyclers in parallel (C1000 Touch Thermal Cycler, Bio-Rad and 2720 Thermal Cycler, Applied Biosystems Waltham, MA, USA). The process involves three distinct temperature stages. Initially, the AAV particles undergo incubation at 37 °C for 30 minutes to treat them with DNase I enzyme. Subsequently, they are subjected to a temperature of 95 °C for 10

minutes to block the DNase I enzyme activity. Finally, the DNA of the rAAV vector is extracted from its capsid by incubating at 70 °C for 10 minutes in lysis buffer. Lastly, samples prepared with both coated and non-coated tools were combined in a single qPCR plate for analysis. The evaluation was carried out utilizing the Applied Biosystems QuantStudio 3 real-time PCR instrument featuring a 96-well, 0.1 mL block configuration (see Figure 2.2.4.A).

2.2.3. Exploring the influence of freeze/thaw cycles in conjunction with coating effects on VG recovery

Quantification qPCR analysis for VG was conducted consecutively three times, utilizing the identical 100-fold diluted stocks, which were subsequently refrozen in sealed cryotube vials at -80 °C after each time from the three consecutive times mentioned above. Freeze/thaw cycles (F/T cycles) were consistently executed under identical conditions, using the same stock samples, to assess day-to-day variations and explore the influence of F/T cycles on AAV suspension within both coated and non-coated containers. In other words, I conducted three rounds of qPCR analysis on the same AAV stock. After each analysis, I froze and thawed the sample before the next round. So basically, I repeated the quantification process three times, with each round separated by freezing and thawing of the AAV sample, all from the same vial. Simultaneously, another set of three tubes, derived from the same 100-fold diluted stock, was sampled independently for VG quantification analysis without undergoing freeze/thaw cycles.

2.2.4. Evaluating rAAV vector adsorption with both coated and non-coated tools

In both the above-mentioned and subsequent experiments, coated tools were employed collectively, meaning all cryotube vials, pipette tips, and qPCR plates were coated. However, in this experiment, the impact of the PHC coating material was investigated by using each coated tool individually. This approach aimed to assess the extent of prevention of nonspecific rAAV adsorption occurring during various qPCR analysis steps, including sample preparation involving pipetting, the use of cryotube vials, and the qPCR plates. The objective was to discern which tool contributed the most to preventing nonspecific vector adsorption when coated. Three distinct VG quantification qPCR analysis experiments were conducted, each involving the coating of only one type of tool—cryotube vials, pipette tips, or qPCR plates (refer to Figure 2.2.4.B).
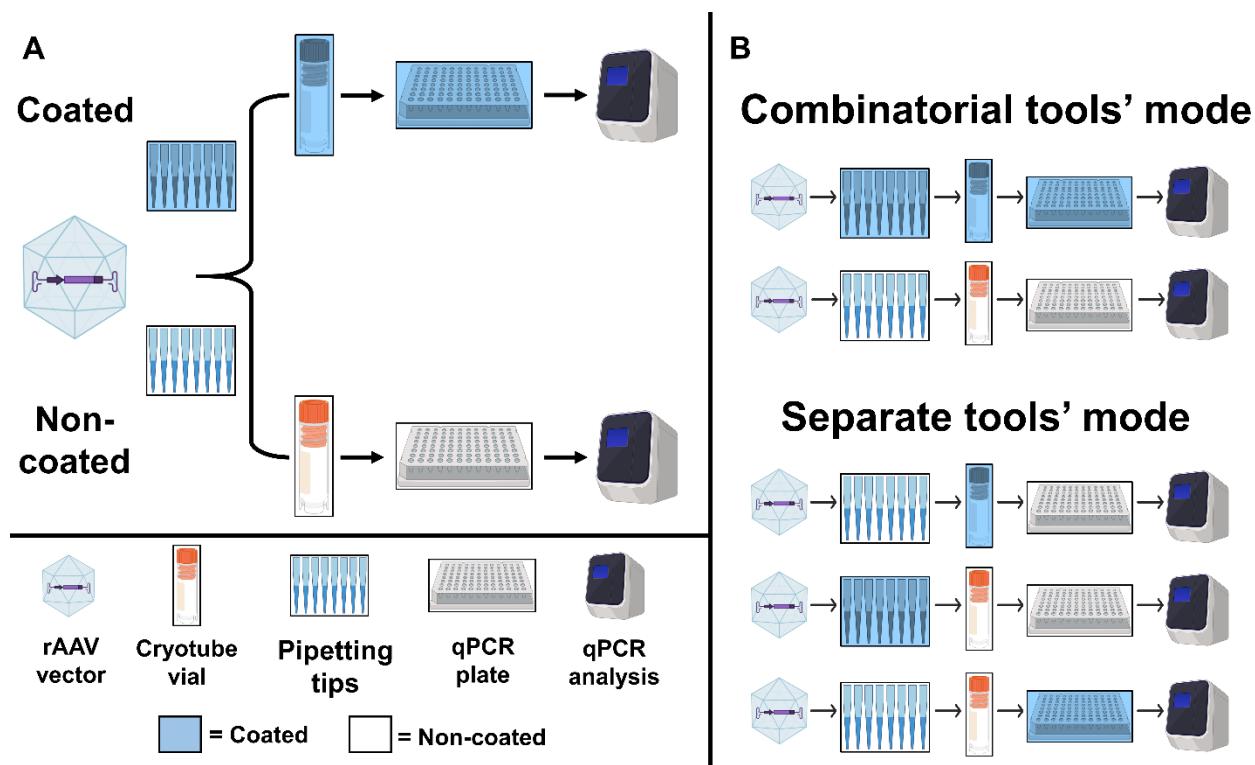
Figure 2.2.4. (A) Schematic diagram presenting the workflow of the qPCR quantification analysis for VG count to examine the effects of the tested PHC coating in minimizing rAAV vector adsorption within the used analytical research tools. **(B)** Illustrative diagram presenting the difference in workflow between the combinatorial and separate tools modes when using coated and non-coated tools for rAAV VG quantification qPCR analysis. In the combinatorial mode, qPCR analysis was conducted using either coated or non-coated tools consistently throughout the experiment. In the separate tools' mode, qPCR analysis was performed using only one type of coated tool in each of the three experiments, with the remaining tools being non-coated. The diagram was created using BioRender.com.

2.2.5. Assessing adsorption with varied concentrations of P-188

Surfactant-free rAAV1 (5.82×10^{12} VG/mL) was subjected to dilution using three different concentrations (0.1%, 0.01%, and 0.001% w/v) of P188 (P2164009, European Pharmacopoeia Reference Standard, Sigma-Aldrich, St. Louis, MO, USA) in PBS. These

surfactant solutions were prepared through serial dilution from a 1% (w/v) stock solution of P188 in PBS. Subsequently, the samples underwent VG quantification through qPCR analysis, utilizing the same foundational experimental procedure outlined earlier, for comparing the performance of PHC-coated and non-coated tools.

2.2.6. Quantifying the reference standard stock (RSS) of rAAV

A reference standard stock of rAAV2 (rAAV2 RSS; ATCC VR-1616, Manassas, VA, USA) with a nominal concentration of 3.28×10^{10} VG/mL was purchased. Subsequently, samples were directly collected onto both coated and non-coated qPCR plates using coated and non-coated pipette tips. The VG concentration was then determined through qPCR analysis employing the previously described rAAV titration kit.

2.2.7. Detecting GFP fluorescence for evaluation of vector transduction activity

HeLaRC32 cells, a stable packaged cell line expressing the rep and cap genes (ATCC® CRL–2972), were seeded at a density of 1.2×10^4 cells/cm2/well in 6-well culture plates (Corning, 3516). The cells were cultured in 3 mL of complete medium which includes Dulbecco's modified Eagle's medium (Sigma-Aldrich, D6429-1L) supplemented with 10% fetal bovine serum (ATCC, 30-2020) and 1% penicillin–streptomycin solution (Thermo Fisher Scientific, 15140122) at 37 °C under a 5% CO2 atmosphere. After 24 hours of incubation, the culture medium was replaced with 1 mL of freshly prepared complete medium. Each well was then transduced with 40 μL of surfactant-free rAAV1 vector stock suspension (2.29×10^{12} VG/mL) and incubated for 6 hours. An additional 2 mL of complete medium were added to each well, and the cells were further incubated for 42 hours, completing a 48-hour transduction period. Three wells of the 6-well plate were

transduced using the viral vector handled with coated tools (pipette tips and cryotube vials), while for the other three wells (control), the vector was handled with non-coated tools. After 48 hours of transduction, green fluorescence was observed using a BZ-X710 All-in-one Fluorescence Microscope (Keyence, Itasca, IL, USA) with excitation at 470–490 nm and emission at 515–550 nm, at 100× magnification. The mean (average) fluorescence intensity coming out of the transduced cells within their pictures was analyzed using ImageJ software (National Institutes of Health, Bethesda, MD, USA).

2.2.8. Alterations in the characteristics of solid surfaces subsequent to the application of PHC coating

The contact angle was measured using a Drop Master Series Contact Angle Meter (DM-701, Kyowa Interface Science, Saitama, Japan). Test tubes made of polypropylene (non-coated or PHC-coated) were cut into pieces of the appropriate size, followed by attachment to the device. When measuring the contact angle of bubbles in water, the polypropylene substrates were placed upside down in water.

The surface zeta potential was measured in Dulbecco's phosphate-buffered saline without calcium and magnesium [D-PBS (–)] using a Zetasizer Nano (Malvern Panalytical Ltd., Malvern, United Kingdom). Polystyrene substrates (non-coated or PHC-coated) were cut to 1 mm × 1 mm and attached to a flat-plate zeta potential measurement unit (ZEN1020, Malvern). The unit was set in a polystyrene cell (10 mm × 10 mm × 45 mm). Polymer latex; micromer 1 µm (micromod, Rostock, Germany) was used as the zeta potential transfer standard.

2.3. Results

2.3.1. Assessing the influence of PHC coating in minimizing rAAV Vector adsorption

QPCR analysis comparing the rAAV1 vector handling with PHC-coated and non-coated tools demonstrated a significant decrease in vector adsorption onto the surfaces of tested tools, including pipette tips, cryotube vials, and qPCR plates. The recovered VG concentrations exhibited a noteworthy difference ($p < 0.01$) between the test and control groups. Additionally, I tried to check whether the PHC coating can have a protective effect against freeze and thaw cycles that are usually known to have a negative effect on rAAV recovery. As illustrated in Figure 2.3.1.(A) that shows a triplicate of rAAV VG quantification analyses without interruption by freeze-thaw (F/T) cycles, the vector VG concentration recovery with coated tools exceeded that observed with non-coated tools by up to 60% of the recovered VG concentration using non-coated tools. Additionally, figure 2.3.1.(B) that shows a triplicate of rAAV VG quantification analyses with interruption by F/T cycles, clearly indicates that after each cycle of freeze and thaw, the tested PHC coating mitigated the negative impact of F/T cycles on the recovered VG count, resulting in a preservation of up to 74% of the lost viral particles.

As depicted in Figure 2.3.1.(C), my aim was to identify the primary step influencing vector adsorption in qPCR analysis. The application of PHC coating markedly reduced rAAV vector adsorption on each of the tested tools. Notably, the coated qPCR plates exhibited the most substantial difference in recovered VG concentration compared to the controls, showcasing a remarkable 95% reduction in lost particles. Coating the qPCR plates resulted in the recovery of 149% of the rAAV nominal concentration, in remarkable contrast to only 7% for non-coated plates. In the case of pipette tips, the coating prevented

adsorption of 92% of rAAV particles, while coated cryotube vials prevented 89% of particles from being adsorbed.
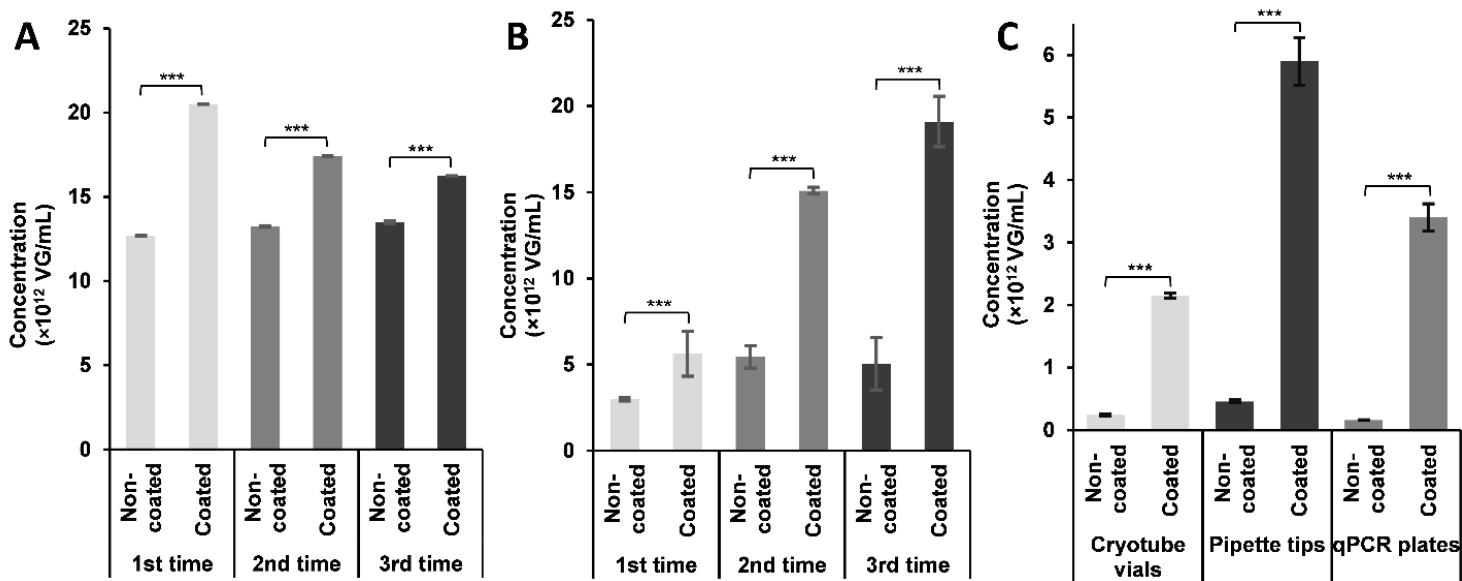

Figure 2.3.1. Quantitative polymerase chain reaction (qPCR) analysis for counting the vector genome (VG) of recombinant adeno-associated virus serotype 1 (rAAV1), comparing samples processed with both coated and non-coated tools. (A) Analyzing the difference in performance between polyionic hydrophilic complex (PHC) coated and non-coated tools, which include pipette tips, cryotube vials, and qPCR plates, all of which had been coated in the combinatorial tools mode (refer to Figure 2.2.4 (B)). 1st time, 2nd time and 3rd time means that the rAAV VG qPCR quantification process was conducted in triplicate without interruption by freeze-thaw (F/T) cycles, using a surfactant-free rAAV1 formulation with a nominal concentration of 5.82×10^{12} VG/mL aliquoted in three different cryotubes. **(B)** Evaluating the performance difference between tools coated with polyionic hydrophilic complex (PHC) and their non-coated counterparts, encompassing pipette tips, cryotube vials, and qPCR plates, all treated in the combinatorial tools mode as illustrated in Figure 2.2.4 (B). 1st time, 2nd time and 3rd time means that the rAAV VG qPCR quantification analysis underwent three successive repetitions, interspersed with freeze-thaw (F/T) cycles, utilizing the same sample of a surfactant-free rAAV1 formulation with a nominal concentration of 2.29×10^{12} VG/mL. This sample underwent freezing and then thawing after each analysis

(C) Assessing the differences in utility between individually treated polyionic hydrophilic complex (PHC)-coated and non-coated tools, such as cryotube vials, pipette tips, or qPCR plates, as depicted in the separate tools mode illustrated in Figure 2.2.4 (B). Coated tools were individually employed in three distinct rAAV VG qPCR quantification analyses, each utilizing a surfactant-free rAAV1 formulation with a nominal concentration of 2.29×10^{12} VG/mL. All data are the mean ± standard deviation (technical replicates $n = 4$). Statistical significance for the coated group compared with that for the non-coated group was determined using the two-tailed unpaired Student's t-test. *$p < 0.05$, **$p < 0.01$, ***$p < 0.001$.

2.3.2. Investigating the impact of PHC coating on minimizing adsorption across various rAAV serotypes and in the presence of P188 surfactant

To investigate whether the reduction in adsorption attributed to the PHC coating was dependent on serotype, the adsorption of three different rAAV serotypes (1, 2, and 8) was quantified. Furthermore, as stated in chapter 1, P188 surfactant is typically included in rAAV formulations in the concentration of 0.001% to reduce the chance of rAAV particles sticking to surfaces they encounter. In this experiment, I wanted to see if adding P188 surfactant affects the PHC coating's ability to minimize the non-specific adsorption of rAAV particles. Basically, I aimed to determine if P188 surfactant could counteract the effects of the PHC coating in preventing rAAV particles from sticking to surfaces. The results indicated that neither the serotype nor the surfactant at this concentration significantly affected the adsorption reduction capability of the PHC coating (see Figure 2.3.2.(A)). Even though all three tested rAAV stocks (1,2, and 8) initially had 0.001% P188 surfactant, there was still a notable statistical distinction in the concentration of VG recovered from tools coated with PHC compared to those left uncoated. Subsequently, the coating material was tested against higher concentrations of the surfactant, and the PHC coating continued to significantly reduce rAAV adsorption (see Figure 2.3.2.(B)).
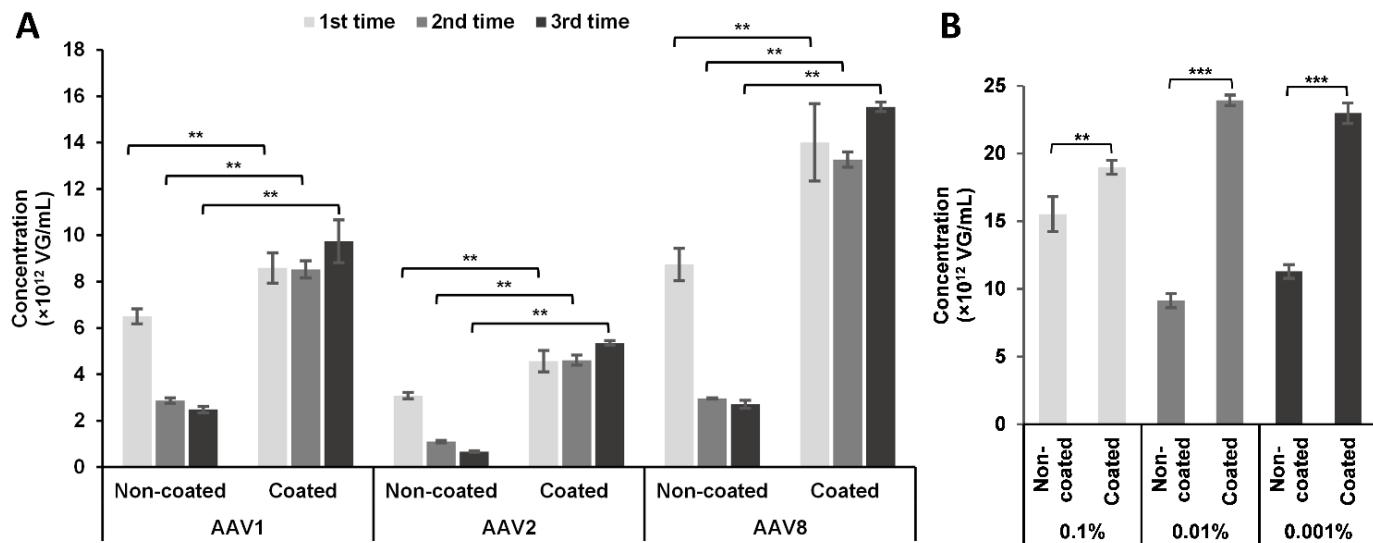
Figure 2.3.2. Quantitative analysis of rAAV VG count by qPCR, investigating the coating's impact across different rAAV serotypes and assessing the surfactant's influence on the coating's role in reducing adsorption. (A) Comparative Analysis of PHC-Coated and Non-Coated Tools, including Pipette Tips, Cryotube Vials, and qPCR Plates, All Subjected to Coating. The Quantification Analysis was Repeated Three Successive Times, Interspersed with F/T Cycles, Utilizing Three Different Serotypes of rAAV: rAAV1 (9.8×10^{12} VG/mL), rAAV2 (6.5×10^{12} VG/mL), and rAAV8 (1.8×10^{13} VG/mL), Each Containing 0.001% P188 Surfactant and Diluted 100-Fold Before Sampling. **(B)** Further Comparison of PHC-Coated and Non-Coated Tools (Cryotube Vials, Pipette Tips, and qPCR Plates), Demonstrating the Impact of Different Concentrations of P188 Surfactant. This Experiment utilized originally Surfactant-Free rAAV1 Formulation with a Nominal Concentration of 5.82×10^{12} VG/mL. All Data Represent Mean ± Standard Deviation (technical replicates n = 4). Statistical Significance for the Coated Group Compared to the Non-Coated Group was Determined Using the Two-Tailed Unpaired Student's t-Test. *p < 0.05, **p < 0.01, ***p < 0.001.

2.3.3. Investigating the influence of PHC coating on the absolute quantification of RSS

As shown in Figure 2.3.3, when quantifying rAAV RSS VG, the application of PHC coating yielded a recovery of 157% of the nominal VG concentration, while the use of non-coated tools resulted in the recovery of nearly the exact nominal VG concentration.
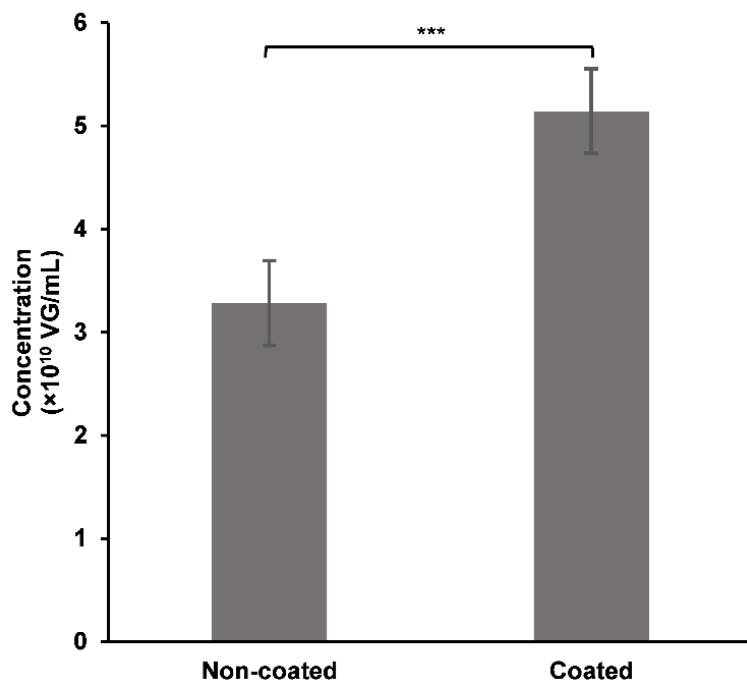
Figure 2.3.3. Quantification of VG count of rAAV2 reference standard stock (RSS) suspension through qPCR. Comparative Analysis of PHC-Coated and Non-Coated Tools (Cryotube Vials, Pipette Tips, and qPCR Plates) in Quantifying rAAV2 ATCC® RSS with a Nominal Concentration of 3.28×10^{10} VG/mL. Results are Presented as Mean ± Standard Deviation (technical replicates n = 4). Statistical Significance for the Coated Group Compared to the Non-Coated Group was Determined Using a Two-Tailed Unpaired Student's t-Test. *p < 0.05, **p < 0.01, ***p < 0.001.

2.3.4. Evaluating the effect of PHC coating on cell line transduction efficiency

The influence of the PHC coating on the transduction efficiency of the rAAV vector was assessed by transducing HeLaRC32 cells with the rAAV1 GFP-expressing vector processed using coated and non-coated tools (pipette tips and cryotube vials) (refer to Figure 2.3.4.1). As illustrated in Figure 2.3.4.2, cells transduced with vector prepared using coated tools exhibited GFP expression with a fluorescence intensity 1.8-fold higher than cells transduced using vector prepared with non-coated tools.
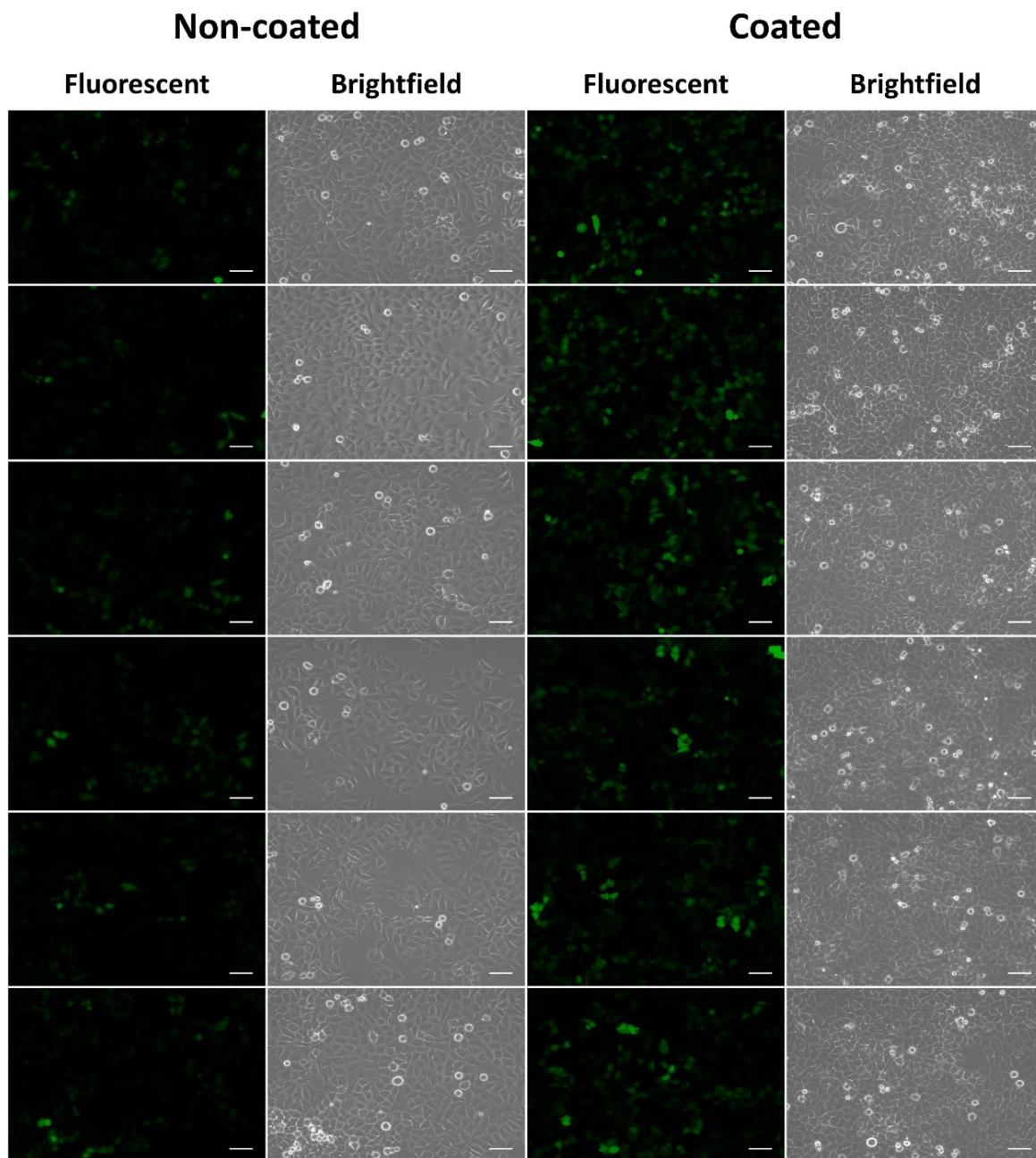
**Figure 2.3.4.1. Representative Fluorescent Images alongside corresponding brightfield images of HeLaRC32 Cells transduced with rAAV1.** Surfactant-free rAAV1 vector with a nominal concentration of 2.29 × 10¹² VG/mL was employed to transduce HeLaRC32 cells using both coated and non-coated tools (cryotube vials and pipette tips). In the Coated group, images depict cells transduced with the rAAV1 vector

processed using coated tools. Conversely, in the non-coated group, images represent cells transduced with the rAAV1 vector processed using non-coated tools. Scale bars indicate 100 μm.
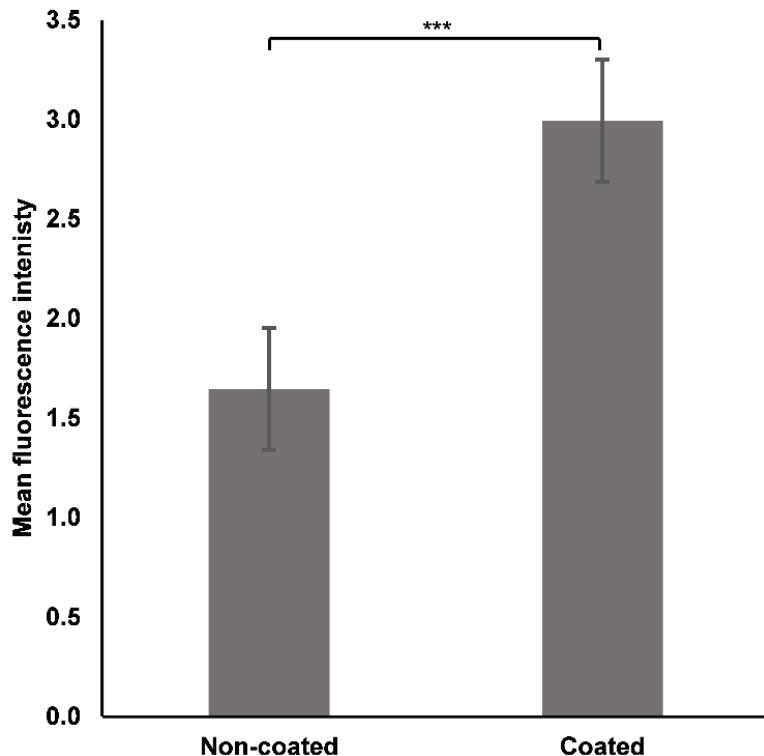
Figure 2.3.4.2. Calculation of mean fluorescence intensity in rAAV1-transduced HeLaRC32 Cells. Values were computed by analyzing fluorescent images acquired from transduced cells through ImageJ software. The comparison focused on the utilization of PHC-coated and non-coated tools (cryotube vials and pipette tips) in rAAV1 cell transduction. Data is presented as the mean ± standard deviation (n = 12 images) (2 images from each well of the used 6-well plate giving 6 images for coated tools and 6 images for the non-coated tools). Statistical significance between the coated and non-coated groups was determined using a two-tailed unpaired Student's t-test. *p < 0.05, **p < 0.01, ***p < 0.001.

2.3.5. Alterations in the characteristics of solid surfaces subsequent to the application of PHC coating

The surface wettability, often denoted as hydrophobicity/hydrophilicity, stands as a critical parameter influencing the biological reaction to substances.[98] I assessed the contact angle of water droplets in the air (using the sessile drop method) or air bubbles in water (employing the captive bubble method) on both coated and non-coated surfaces. Both techniques are widely utilized for measuring hydrophobicity/hydrophilicity and are considered complementary to each other.[99] [100] As depicted in Figure 2.3.5, the sessile drop method did not distinctly reveal the hydrophilic properties of the coating. Conversely, the captive bubble technique demonstrated that surfaces treated with the coating material exhibited greater hydrophilicity compared to non-coated surfaces. These findings suggest that the PHC coating film exhibited a hydrophilic state in water or in aqueous solutions. Additionally, the results showed that the coated substrate surface zeta potential has changed to almost zero after coating.
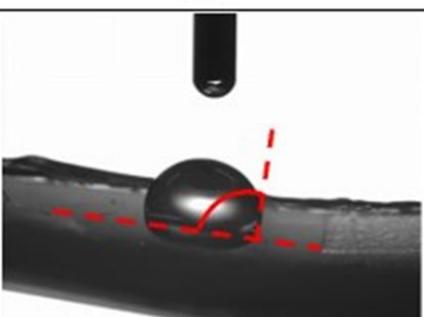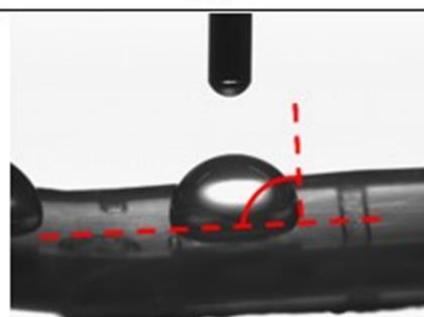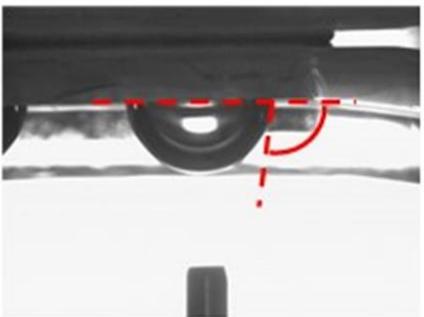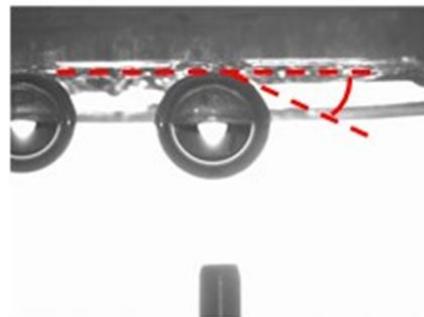
	Non-coated	PHC-coated
Contact angle of water droplets in air (sessile drop method)	94°	90°
Contact angle of air bubbles in water (captive bubble method)	96°	28°
Surface Zeta potential	-59 mV	-4 mV

Figure 2.3.5. Alterations in the characteristics of solid surfaces subsequent to the application of PHC coating. The hydrophilicity/hydrophobicity of the coating was assessed by measuring the contact angles for both non-coated and PHC-coated surfaces using both the sessile drop and captive bubble methods. Surface charge also was assessed for both non-coated and PHC-coated surfaces.

2.3.6. Investigating the influence of pH on the measured contact angles for the coated and non-coated tools

Contact angles were measured using the captive bubble method for both PHC-coated and non-coated surfaces across a wide range of pH values. The results revealed that pH has no influence on the hydrophilicity of the coated surfaces or the comparable hydrophobicity of the non-coated surfaces. And the measured contact angles remain almost constant across the tested range of pH values.
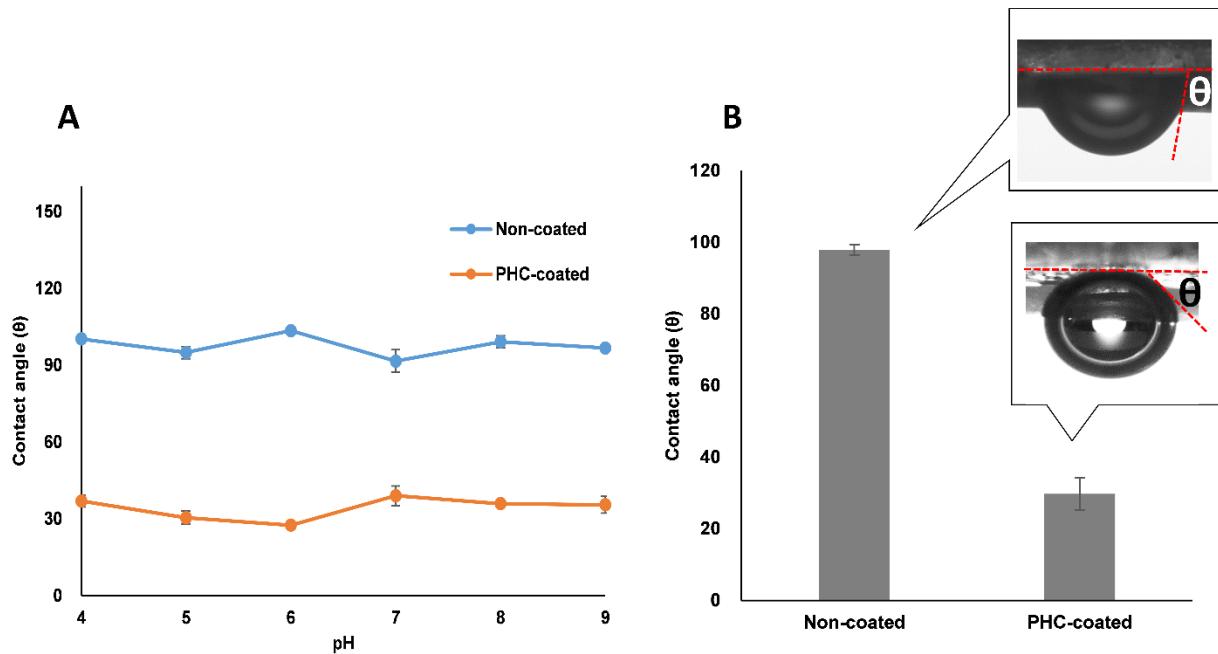
Figure 2.3.6. Determination of the contact angle for surfaces with and without PHC coating using the captive bubble method across the pH spectrum from 4 to 9. (A) Contact angle measurements across pH 4 to 9 displayed no significant difference in values regardless of solvent pH. (B) Average contact angle values for both PHC-coated and non-coated surfaces, indicating the measured angle (θ) as the contact angle.

2.3.7. Investigating difference in water evaporation between PHC coated and non-coated tools

A phenomenon observed during work is that the water meniscus in PHC-coated tools has a more concave shape compared to the water meniscus in non-coated tools as seen in figure 2.3.7.1. This results in an increase in the surface area of the water meniscus in the coated tools that could lead to a difference in water evaporation among coated and non-coated tools. Therefore, I conducted an experiment designed to examine the amount of water evaporation among coated and non-coated tools. The findings indicate that the coated tool experiences a higher rate of water evaporation over a fixed period of time compared to the non-coated tools as seen in figure 2.3.7.2.
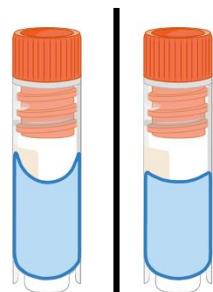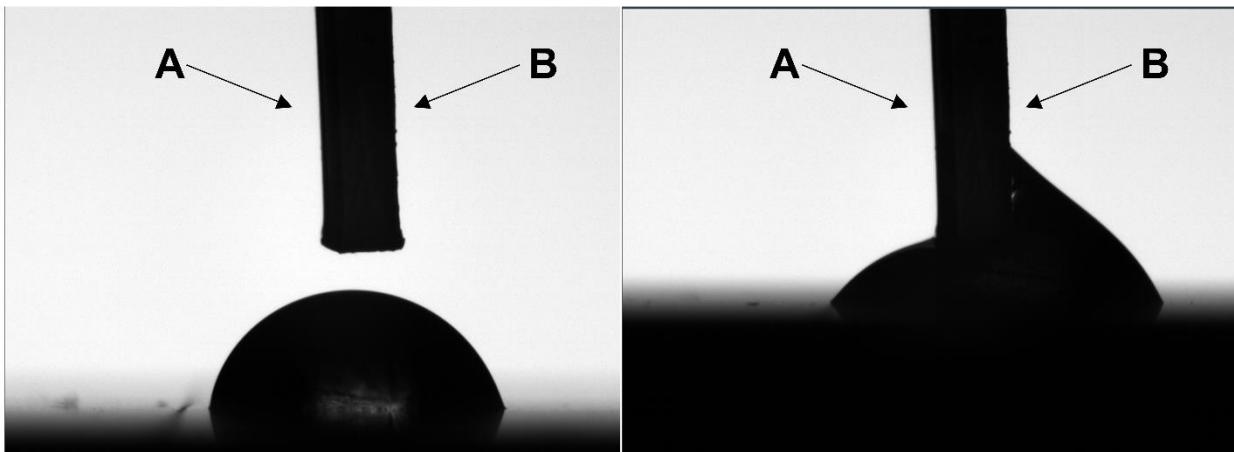
Figure 2.3.7.1. Visual representation and actual photographs showing the impact of the examined PHC coating on the water's surface. (1) Visual representation: Side (A) Coated cryotube vial and four coated wells of a qPCR plate all filled with water. **Side (B)** Non-coated cryotube vial and four non-coated wells of a qPCR plate all filled with water. Adhesion of water molecules to the container wall was considerably higher for the coated cryotube vials and qPCR plates than the non-coated vials and plates. This is due to the hydrophilic properties of the coating material, which results in the migration of water molecules onto the coated walls, leading to extension of the meniscus to a larger surface area. Therefore,

the water evaporation rate is higher. With respect to my experimental design, the water evaporation rate is higher from qPCR plates than from cryotube vials. qPCR plates are subject to evaporation during the whole procedure of sample preparation until the plates are put into the qPCR instrument for analysis; however, cryotube vials are subject to evaporation only during the pipetting and sampling steps, which constitute a short time period compared with the time taken for the whole analysis. The diagram was created using BioRender.com.

(2) Images: A piece 4 mm × 20 mm was cut off a cryotube vial, and then, by means of an optical tensiometer (Attension theta Flex, Biolin Scientific®, Gothenburg, Sweden), pictures of a 30-µL ultrapure water drop meniscus were captured showing the effect of the tested coating on the water surface. **Side (A)** The non-coated surface of the cut-off piece (the outer surface of the cryotube). **Side (B)** The coated surface of the cut-off piece (the inner surface of the cryotube). The picture on the left shows the water drop and the cryotube cut-off piece just before touching each other, while that on the right shows them after immersion of the cut-off piece into the water drop. It is clear that the hydrophilicity of the tested coating material increased the surface area of the water meniscus through the higher adhesion force between the coating and the water molecules and then by the cohesive force between the water molecules. This all results in an increased water surface area available for evaporation.
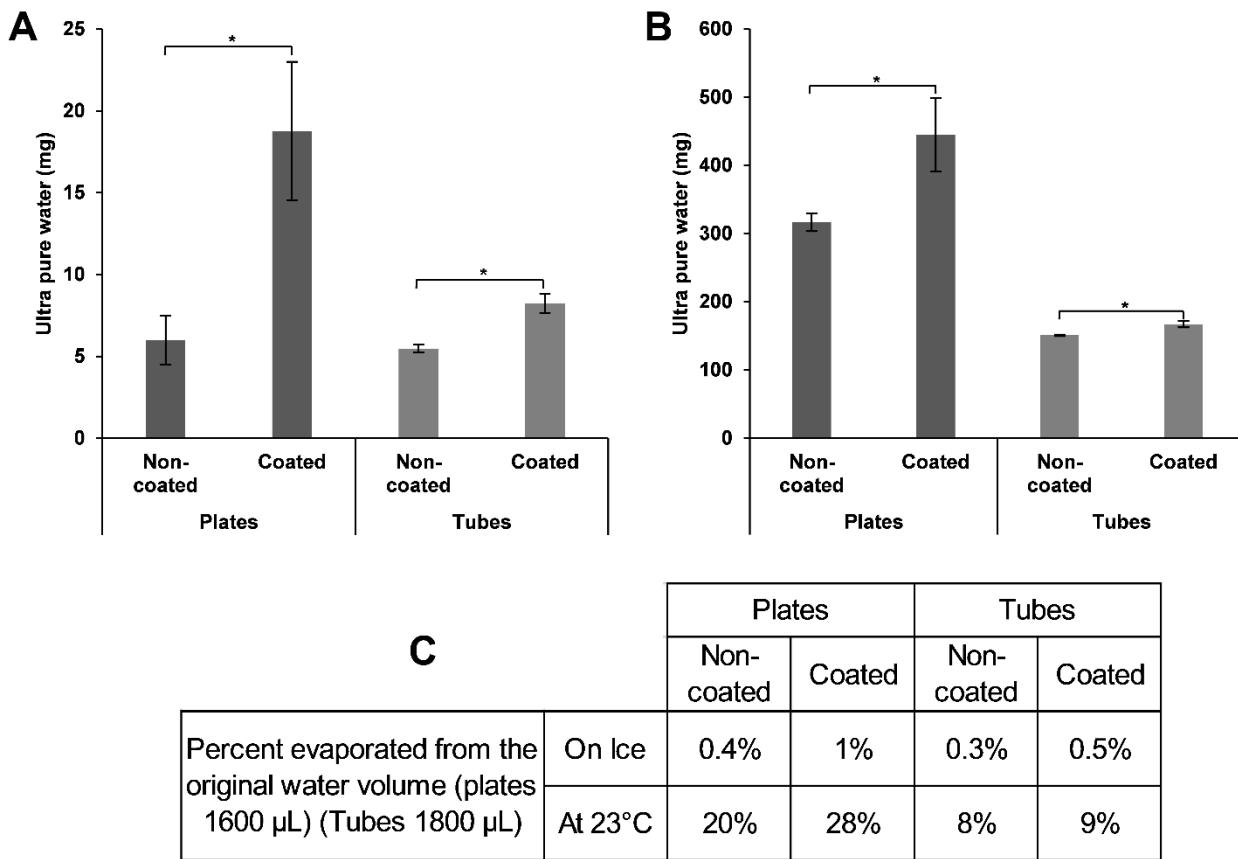
Figure 2.3.7.2. Differential water evaporation comparison between qPCR plates and cryotube vials with and without the PHC coating. Coated and non-coated qPCR plates were each filled with 1600 μL of ultrapure water; the 1600 μL were divided into 16 wells in each plate such that each well contained 100 μL (wells 1A to 1H and 12A to 12H). Coated and non-coated 1.5-mL cryotube vials were each filled with 1800 μL of ultrapure water. Both plates and vials were weighed using a balance (AP125WD, Shimadzu, Kyoto, Japan) at time = 0, then subjected to evaporation for 5 h and reweighed. The weight of evaporated water was obtained as t_0 weight $-$ t_5 weight. **(A)** Plates and vials were subjected to evaporation while sitting on ice. **(B)** Plates and vials were subjected to evaporation while sitting at room temperature (23°C). **(C)** Percentages of evaporated water volume compared with those of the original volume before evaporation. Data are depicted as the mean ± standard deviation (n = 3). Statistical significance for the coated group

compared with those for the non-coated group was determined using the two-tailed unpaired Student's t-test. *p < 0.05, **p < 0.01, ***p < 0.001.

2.4. Discussion

I observed that applying the coating enabled the recovery of a significant proportion of vector particles that typically undergo adsorption. When utilizing PHC-coated tools for sample processing, the recovery of rAAV VG was notably 50% to 95% higher compared to the processing with non-coated controls (refer to Figure 2.3.1). The impact of preventing additional viral particles from adsorption was evident in achieving a higher transduction efficiency, as demonstrated in Figures 2.3.4.1 and 2.3.4.2.

Furthermore, I sought to replicate the dilution process commonly incorporated in the administration of rAAV drug products throughout the whole experiments, whether through bolus injection, as seen in the Luxturna case,[79] or by an intravenous infusion, as for Zolgensma.[101] I examined the impact of each individually coated tool (pipette tips, cryotube vials, or qPCR plates) on the adsorption of viral particles. As depicted in Figure 2.3.1.(C), the most significant difference in rAAV adsorption between coated and non-coated tools was observed for the qPCR plates. This finding suggests that the mechanism of non-specific rAAV adsorption is time-dependent, aligning with findings from previous studies.[54] [55] This is attributable to the fact that, in the context of all the experimental procedures, the rAAV particles spent the most extended duration in the wells of the qPCR plates. The substantial difference in rAAV adsorption observed between the use of coated and non-coated pipette tips may be attributed to the frequency of sample pipetting, which encompasses sample transfer, preparation, and mixing (a critical step for accurate AAV analysis).[78] [102] The possibility of cumulative particle adsorption arises when pipetting is performed multiple times. Pipette tips are the most frequently utilized tool in qPCR analysis, with numerous tips often required for a single analysis (typically involving one

qPCR plate and one cryotube vial). As a result, the use of coated tips led to the highest AAV particle recovery. Therefore, I particularly recommend the application of the tested PHC coating to pipette tips. The cryotubes exhibited the least amount in rAAV adsorption, suggesting that the duration of contact between the rAAV vector and the tool's surface is minimized in the thawed state, accompanied by reduced movement, such as pipetting or mixing. These findings lend support to the hypothesis that non-specific adsorption predominantly contributes to the loss of rAAV vectors during various experimental steps. The observed trend underscores the significance of mitigating adsorption concerns, particularly in tools with prolonged vector interaction, to enhance the overall recovery of AAV particles.

The data shown in Figures 2.3.1.(A) and 2.3.1.(B) revealed a noteworthy trend when employing the same rAAV stock for sequential experiments with intermittent F/T cycles. When non-coated tools were utilized, a significant decline in the recovered VG count was evident among the three successive analyses denoted as 1st time, 2nd time and 3rd time. In contrast, the use of coated tools among the three successive analyses denoted as 1st time, 2nd time and 3rd time exhibited an increasing VG count. This phenomenon may be attributed to several factors. The surfaces treated with the coating material exhibited hydrophilicity, as evidenced by the findings from the contact angle and surface wettability assessments (Figure 2.3.5). According to Alexander et al., surfaces with higher hydrophilicity tend to have freezing temperatures closer to that of water, whereas hydrophobic surfaces exhibit decreased freezing temperatures below that of water.[103] In addition, a prior study suggested that the F/T process induces the aggregation of rAAV particles.[41] Thus, I hypothesize that within non-coated tools, the rAAV formulation

undergoes non-uniform freezing, subjecting vector particles to increased stress during F/T cycles. This phenomenon may explain the observed decrease in VG count (Figure 2.3.1.(B)) compared to VG recovery experiments without interspersed F/T cycles (Figure 2.3.1.(A)). Consequently, my belief is that the PHC coating serves a protective role, mitigating the impact of freeze/thaw cycles during the storage of rAAV vectors. The increase in VG count during successive analyses in Figure 2.3.1.(B) and Figure 2.3.2.(A) when using coated tools primarily stems from the robust adhesion force between water molecules and the highly hydrophilic coating material. This interaction, coupled with the cohesion force among water molecules, encourages water molecules in the rAAV suspension to adhere to and migrate over the surfaces of tubes and qPCR plates. (see Figures 2.3.7.1 and 2.3.7.2) As a result, the available surface area for evaporation increases, leading to the observed rise in VG concentration after each analysis. This phenomenon could also elucidate the significant difference in the recovered VG count between coated and non-coated qPCR plates (Figure 2.3.1.(C)).

Examining the outcomes shown in Figure 2.3.1.(B) notable fluctuations in the recovered VG concentration in both cases of coated and non-coated tools among the three successive times of analysis while in Figure 2.3.2.(A) relatively consistent reproducibility in the recovered VG concentration in both cases of coated and non-coated tools were evident in the successive experiments conducted. This variability might be attributed to the inclusion of P188 surfactant in the rAAV vector formulations utilized in the experiments illustrated in Figure 2.3.2.(A). This surfactant is typically employed to ensure a uniform and quantitative recovery of AAV vector.[51] The data presented in Figure 2.3.2.(B) indicated an increase in the percentage recovery of rAAV VG with higher concentrations

of P188 surfactant, aligning with existing literature[104] reporting a two- to tenfold reduction in AAV count in the absence of P188. Additionally, my study demonstrated that the PHC coating facilitated the recovery of a higher concentration of rAAV VG even in the presence of a comparatively elevated surfactant concentration. However, the use of P188 mitigated the difference in percentage recovery between coated and non-coated tools as seen in Figure 2.3.2.(B) especially in the concentration of 0.1% P188. In Figure 2.3.5., the captive bubble method distinctly demonstrated the pronounced hydrophilicity of the PHC coating. The conventional sessile drop method may not attain measurable equilibrium values with water droplets.[105] Moreover, maintaining fully hydrated conditions throughout the experiment is challenging, [106] resulting in inaccurate outcomes.

Chapter 3

Exploring the mechanism of action of PHC coating in conjunction with the fundamental mechanism of rAAV adsorption

3.1. Introduction

While various mechanisms underlie the surface adsorption of protein molecules, including intra-molecular forces, hydrophobicity, ionic interactions, and electrostatic interactions,[45] [107] the precise mechanism of rAAV surface adsorption remains to be fully elucidated. This chapter aimed firstly to determine the mechanism of action of the PHC coating in minimizing the non-specific adsorption of rAAV particles. Secondly, it aimed to investigate the basic mechanism of non-specific surface adsorption of rAAV by comparing Polypropylene that is characterized by a hydrophobic negatively charged surface,[108] with glass, which possesses a hydrophilic negatively charged surface.[109] [110] The study sought to examine both hydrophobic and electrostatic interactions by manipulating the surface charge of rAAV vector particles through adjustments in pH values. Additionally, the investigation extended beyond rAAV1 to include rAAV9, which has gained increased attention in the rAAV research community. Notably, rAAV9 has already been introduced to the market as a drug product (Zolgensma) for treating Spinal Muscular Atrophy (SMA)[111] and is the subject of numerous phase-2 clinical trials, including those focusing on Lysosomal Diseases.[40]

3.2. Materials and methods

3.2.1. Investigating the pH dependent mode of action of PHC coating in mitigating non-specific adsorption of rAAV through changing pH

According to Gomori,[112] citrate buffer was prepared at two different pH values, 5.6 and 6.2, using citric acid (035-03495, citric acid monohydrate, Wako, Japan) and sodium citrate (191-01785, trisodium citrate dihydrate, Wako) in 155 mM NaCl (191-01665, sodium chloride, Wako). Surfactant-free rAAV1 (5.82×10^{12} VG/mL; Manufacturing Technology Association of Biologics) was diluted 100-fold in 1× PBS (pH 7.4; 10010023, Thermo Fisher Scientific) originally containing 155 mM NaCl, or in the abovementioned citrate buffers. Then, each of the three different pH rAAV1 stocks was divided into coated and non-coated vials. Finally, the VG concentration was determined by qPCR analysis using the rAAV titration kit.

3.2.2. Investigation of rAAV basic mechanism of adsorption

rAAV 9 with a nominal concentration of 3.02×10^{12} VG/mL that is basically containing 0.001% P188 surfactant was provided by the rAAV manufacturing team within the laboratory. To make rAAV9 in our lab, the production team has combined a plasmid containing yellow fluorescent protein (YFP), pAAV-Rep-Cap (serotype 9), and pAd helper and transfected them into VPC 2.0 cells (A49784, Thermo Fisher Scientific) using FectoVIR-AAV transfection reagent (101000004, Polyplus). The cells were then cultured in a flask. After 4 days, they collected the medium and cell lysate, filtered them, and purified them using AAVX prepacked columns (A36652, POROS™ GoPure™ AAVX Pre-packed Column, 0.5 x 5 cm, 1 mL) through affinity chromatography. Then they used cesium chloride ultracentrifugation to separate full and empty particles, collecting the full

particle fractions which were then dialyzed in 1× PBS buffer with 200 mM NaCl and 0.001% poloxamer 188. Dialysis was performed to eliminate the surfactant form the rAAV formulation using Slide-A-Lyaer 10 Dialysis cassette G2 (87729, Thermoscientific). To obtain a surfactant-free vector, firstly rAAV 9 sample of 1 mL was dialyzed in 100 mL of (1x) PBS buffer 7.4 pH for a first round lasting for 3 hours then the dialysis buffer was discarded and a second round of dialysis with fresh 100 mL buffer was performed for an overnight time. Dialysis was done in a glass beaker and a magnetic stirrer (Masuda model SM-15C). After dialysis was finished rAAV sample was kept in -80 °C.

PBS buffer was adjusted at three different pH points (4.8, 5.9 and 8) using 1N HCL or 1N NaOH solutions. rAAV sample was thawed and diluted 100-folds in each of three polypropylene tubes (Eppendorf, 0030120.086) and three glass vials (Daiwa special glass, 16x33 VIST) with rubber stoppers (Maruemu Corporation, 1306-02) each containing a 1mL of PBS buffer with one of the previously mentioned pH points. Samples were kept for 4 hours on ice to allow adsorption and then samples were taken for a qPCR analysis using the titration kit as mentioned earlier.

3.3. Results

3.3.1. Investigating the pH dependent mode of action of PHC Coating in mitigating non-specific adsorption of rAAV through changing pH

At pH 6.2, there was no statistically significant distinction in the recovery concentrations of rAAV1 VG between tools that were coated and those that were non-coated (refer to Figure 3.3.1), aligning with the isoelectric point (pI) range of AAV1, which is 6.2–6.4.[113] Nevertheless, at pH 5.6 or 7.4, the recovery concentrations of VG were notably higher when utilizing coated tools compared to the use of non-coated tools. These findings underscore the influence of electrostatic charge repulsion, whether involving positively charged rAAV1 particles at pH 5.6 or negatively charged ones at pH 7.4, and the zwitterionic PHC polymer coating under examination.
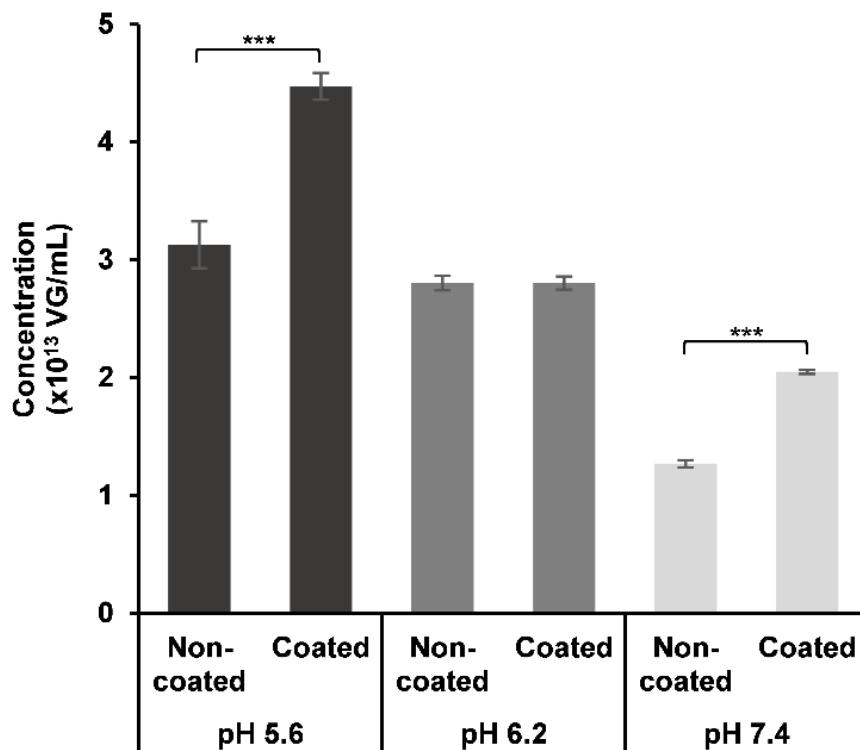
Figure 3.3.1. Investigating the pH dependent mode of action of PHC Coating in Mitigating Non-Specific Adsorption of rAAV1 through changing pH. A pairwise examination of the utilization of PHC-coated and non-coated tools, encompassing pipette tips, cryotube vials, and qPCR plates. The analysis was conducted at three distinct pH values: 5.6 and 6.2 (utilizing citrate buffer) and 7.4 (utilizing PBS). The quantification analysis was performed using a surfactant-free rAAV1 formulation with a nominal concentration of 5.82×10^{12} VG/mL. Data are the mean ± standard deviation (technical replicates $n = 4$). Statistical significance for the coated group compared with that for the non-coated group was determined using the two-tailed paired Student's t-test. *$p < 0.05$, **$p < 0.01$, ***$p < 0.001$.

3.3.2. Investigation of rAAV basic mechanism of adsorption

In this experiment, I selected three different pH values, 5.9 which is the pI of AAV9 [114] [115] alongside with lower and higher values 4.8 and 8 respectively. Results in figure 3.3.2 showed that the highest recovery of rAAV particles has been achieved at pH 8 in both polypropylene and glass. However, glass has an extra higher recovery of vector particles. Although the overall recovery of rAAV vector at pH 5.9 and pH 4.8 was low in both glass and polypropylene, glass still has a higher recovery compared to polypropylene.
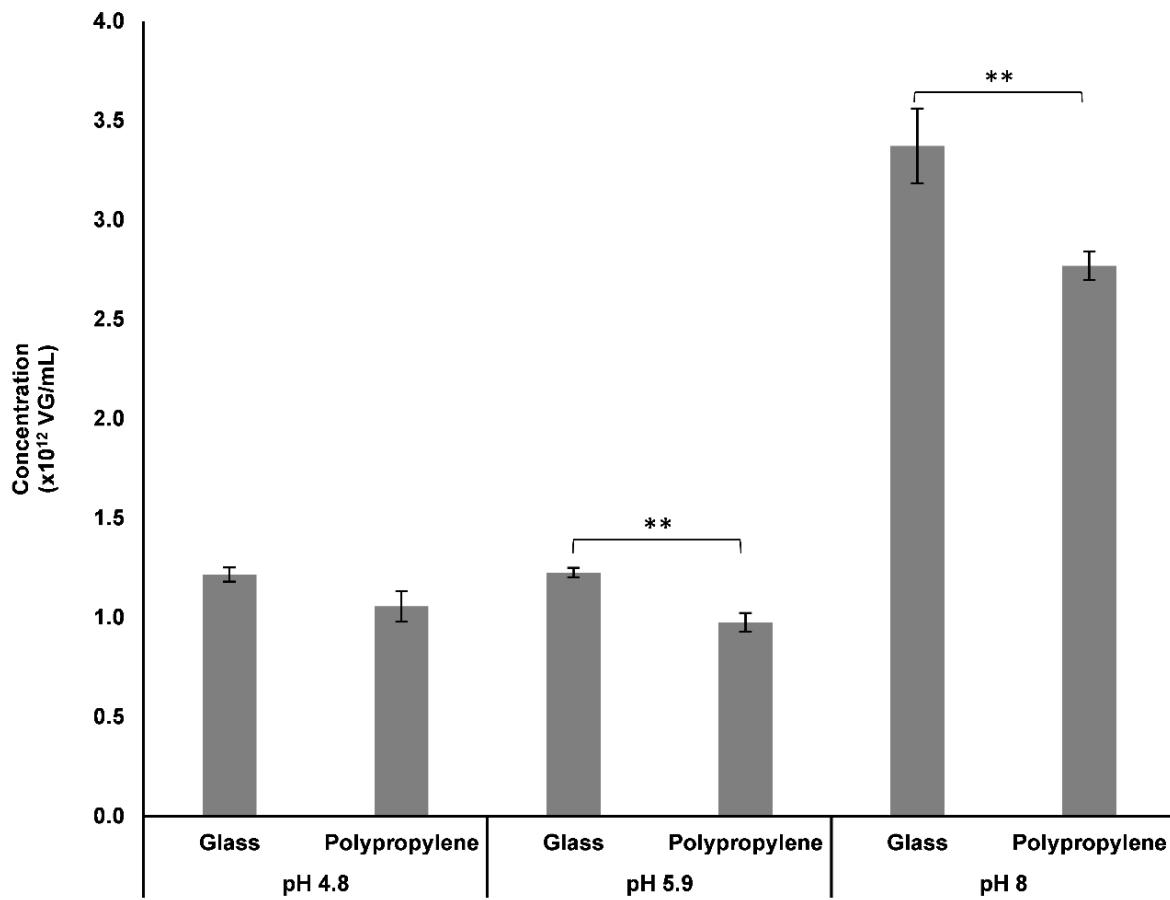
Figure 3.3.2. Investigation of rAAV basic mechanism of adsorption. A pairwise comparison between polypropylene and glass at three different pH points (4.8, 5.9 and 8) using polypropylene tubes and glass

vial. The qPCR VG recovery analysis was made using a surfactant-free rAAV9 with a nominal concentration of 3.02 × 10^{12} VG/mL. Data are the mean ± standard deviation (technical replicates n = 4). Statistical significance for the coated group compared with that for the non-coated group was determined using the two-tailed paired Student's t-test. *p < 0.05, **p < 0.01, ***p < 0.001.

3.4. Discussion

With contrast to chapter 2 experiments that were performed in pH 7.4 only, rAAV vector stocks employed in this chapter were suspended in different pH values. As depicted in Figure 3.3.1., this experiment was specifically designed to examine the pH dependent mode of action of PHC Coating in mitigating non-specific adsorption of rAAV by altering pH values, which influences the surface charge of rAAV particles. pH values of 5.6, 6.2, and 7.4 were employed for this purpose. The isoelectric point (pI) values of AAV1 is between 6.2 and 6.4,[113] and, as per Merten and Al-Rubeai, the majority of viral vectors, including AAV, exhibit a negative charge at a pH of 7.4, given that their pI values are below this threshold.[116] Consequently, rAAV1 particles were nearly neutral at pH 6.2 and carried a positive charge at pH 5.6. The findings presented in chapter 2 Figure 2.3.5. indicated that the absolute surface charge of PHC-coated surfaces was significantly lower than that of non-coated surfaces, approaching nearly zero. The results shown in Figure 3.3.1. suggest that the primary factor contributing to the reduced adsorption of rAAV onto coated tools was the electrostatic interaction between charged rAAV vector particles (at pH 5.6 or 7.4) and the phosphate or amine groups present in the zwitterionic PHC coating. I also posit that the considerable hydrophilicity observed in the tested coating (chapter 2 Figure 2.3.5.) decreased the surface free energy, facilitating the suspension of the relatively hydrophobic rAAV particles between the coated surface and the surrounding liquid, preventing their preferential adsorption onto the surface. To gain a more in-depth understanding of the mechanism behind rAAV adsorption, an experiment shown in Figure 3.3.2. was devised. Using rAAV9, a serotype different from the one in the experiment shown in Figure 3.3.1, and employing glass, which has an originally hydrophilic and

negatively charged surface, in contrast to polypropylene, which has an originally hydrophobic and negatively charged surface. As shown in Figure 3.3.2., at pH 8, where rAAV9 particles are negatively charged (pH higher than the pI), the highest particle recovery was achieved in both glass and polypropylene, indicating the influence of electrostatic interactions through repulsion between the negatively charged rAAV9 particles and both negatively charged glass and polypropylene. While glass had a higher recovery than polypropylene possibly due to its hydrophilicity. However, at pH 5.9, which is the pI of rAAV9 that renders the rAAV9 particles to be almost non-charged, glass had a little higher recovery concentration compared to polypropylene possibly due to only its hydrophilicity. Furthermore, at pH 4.8, the attraction between positively charged rAAV9 particles (pH lower than the pI) and both negatively charged glass and polypropylene resulted in a notable decrease in VG recovery in both polypropylene and glass and also resulted in a non-significant difference between them, although the influence of glass's hydrophilicity could still be seen in a little higher recovery than polypropylene. In conclusion, both electrostatic and hydrophobic interactions may contribute to rAAV9 non-specific adsorption. However, electrostatic interactions are predominant when rAAV9 particles carry a charge as seen in both cases at pH 8 and pH 4.8.

Chapter 4

General Discussion and future perspectives

One of the main obstacles in the manufacturing and analytical processes of rAAV is the undesired binding of the vector to commonly encountered surfaces. This phenomenon plays a substantial role in the depletion of vectors, consequently elevating the costs and resources invested in both the production of the ultimate drug product and the research and development endeavors. Effectively minimizing this adsorption is essential for substantial savings in both cost and effort. Additionally, ensuring the precise clinical administration of the accurate dose is crucial for maintaining patient safety. In this investigation, I applied a PHC polymer coating to the surfaces of tools utilized in storing and quantifying rAAV vectors. This coating emerged as a consistent and efficient method for reducing the non-specific adsorption of the rAAV vector, surpassing the effectiveness of the typically added surfactant. The highly effective suppression of AAV vector adsorption can be attributed to the hydrophilicity and to the polyionic properties of the applied coating, even though the net surface charge, as indicated by the zeta potential at physiological pH, is nearly zero.

The outcomes obtained with the PHC coating in this investigation suggest that achieving absolute quantification of VG is a challenging task, and the determined values are inherently relative and dependent on the chosen methodology. The application of the PHC coating led to a 57% increase in the recovered VG count compared to the nominal concentration of the RSS. Conversely, utilizing tools conforming to the rAAV RSS specifications provided by the manufacturer (ATCC®), such as uncoated polypropylene

tubes,[117] [118] resulted in obtaining almost the nominal concentration stated by the manufacturer. In line with findings by Lock et al. and Ayuso et al., the qPCR analysis for rAAV VG quantification exhibits significant variability both within the same laboratory and across different laboratories, with variations reaching up to 2 logs.[59] [119] Variability in qPCR results can be attributed to factors such as the generation of standard curves, differences in instruments, variations in reaction composition, errors in calculations and error propagation, subsampling errors, and human operator errors encompassing sample treatment, handling, and nucleic acid extraction.[120] [121] Moreover, errors due to pipetting can result in coefficient of variation shifts between 5% and 37%.[122] The variations observed in the recovered rAAV values, especially in non-RSS stock solutions, can be attributed to several factors, underscoring the significance of standard stock solutions in ensuring accuracy in rAAV qPCR analyses. However, it is noteworthy that modern techniques such as digital droplet PCR (ddPCR) exhibit advantages over qPCR in terms of precision and robustness, thereby mitigating interlaboratory variations. ddPCR's independence from a standard curve, prior DNA extraction, or reference standard materials,[91] coupled with its reduced sensitivity to inhibitors in formulation components, contributes to its enhanced reliability.[123]

As a future perspective, the implementation of the PHC coating trial has paved the way for reducing non-specific surface adsorption of rAAV by introducing the concept of coating surfaces that come into contact with it. Therefore, other coatings could be developed for facing the same issue but with more enhanced activity. Moreover, the concept of coating could be extended beyond polypropylene surfaces to encompass a broader range of materials. Additionally, the PHC coating efficacy could be evaluated on medical apparatus

such as tubing and administration devices. Further exploration into the general mechanisms underlying rAAV adsorption, as well as the specific mechanisms through which the PHC coating mitigates this adsorption, holds promise. Such investigations could delve deeper into factors related to rAAV formulation, such as the presence of salts. These salts may either screen or shield electrostatic interactions; however, they could also potentially lead to the salting out of rAAV particles, thereby increasing aggregation and adsorption.

Conclusions

This study demonstrates that employing a PHC polymer coating with zwitterionic hydrophilic properties effectively minimizes non-specific adsorption of rAAV vectors to surfaces. Also, it demonstrates that both electrostatic and hydrophobic interactions contribute to rAAV non-specific adsorption. However, electrostatic interactions are predominant when AAV particles carry a charge. The PHC coating functions through its dual characteristics of hydrophilicity and zwitterionic properties. Hydrophilicity serves to reduce hydrophobic interactions between rAAV particles and hydrophobic surfaces, while the zwitterionic property diminishes electrostatic attraction forces between rAAV particles and charged surfaces. The coating offers a potential substitute for surfactants, displaying consistent effectiveness and overcoming the issue of dilution commonly associated with surfactants. This innovative coating holds promise in preventing significant vector particle adsorption and shielding against the adverse impact of F/T cycles on preserved AAV formulations. It presents considerable potential for widespread application in AAV storage, shipment, and quantification. Nevertheless, additional research is imperative before incorporating the coating into clinical applications.

Acknowledgments

I would like to express my gratitude to Prof. Susumu Uchiyama and Assoc. Prof. Tetsuo Torisue for patiently guiding me towards the end of my journey. They never gave up pushing me forward and supporting me all the time.

I would like to acknowledge Prof. Eiichiro Fukusaki and Prof. Hajime Watanabe for their invaluable guidance, insightful feedback, and meticulous review of my thesis. their valuable input and constructive criticism have contributed immensely to the refinement of my thesis.

I would like to thank Professor Takeshi Omasa for his technical assistance.

I would like to acknowledge Nissan chemical corporation for their fruitful collaborations.

Sincerely and deeply, I would like to thank my big family; Dad, Mom, and sisters and especially my wife for her continued support and patience besides, thanking my close friend Karim for his continued support.

References

[1]   I.M. Verma, M.D. Weitzman, GENE THERAPY: Twenty-First Century Medicine, Https://Doi.Org/10.1146/Annurev.Biochem.74.050304.091637 74 (2005) 711–738. https://doi.org/10.1146/ANNUREV.BIOCHEM.74.050304.091637.

[2]   G.M. Rubanyi, The future of human gene therapy, Mol. Aspects Med. 22 (2001) 113–142. https://doi.org/10.1016/S0098-2997(01)00004-8.

[3]   M.F. Naso, B. Tomkowicz, W.L. Perry, W.R. Strohl, Adeno-Associated Virus (AAV) as a Vector for Gene Therapy, BioDrugs 31 (2017) 317–334. https://doi.org/10.1007/s40259-017-0234-5.

[4]   R. Ni, J. Zhou, N. Hossain, Y. Chau, Virus-inspired nucleic acid delivery system: Linking virus and viral mimicry, Adv. Drug Deliv. Rev. 106 (2016) 3–26. https://doi.org/10.1016/j.addr.2016.07.005.

[5]   M.A. Kay, J.C. Glorioso, L. Naldini, Viral vectors for gene therapy: the art of turning infectious agents into vehicles of therapeutics, Nat. Med. 7 (2001) 33–40. https://doi.org/10.1038/83324.

[6]   D. Bouard, N. Alazard-Dany, F.L. Cosset, Viral vectors: from virology to transgene expression, Br. J. Pharmacol. 157 (2009) 153–165. https://doi.org/10.1038/BJP.2008.349.

[7]   S. Munier, I. Messai, T. Delair, B. Verrier, Y. Ataman-Önal, Cationic PLA nanoparticles for DNA delivery: Comparison of three surface polycations for DNA binding, protection and transfection properties, Colloids Surfaces B Biointerfaces 43 (2005) 163–173. https://doi.org/10.1016/J.COLSURFB.2005.05.001.

[8]   W. Walther, U. Stein, Viral Vectors for Gene Transfer, Drugs 2000 602 60 (2012) 249–271. https://doi.org/10.2165/00003495-200060020-00002.

[9]   T.A. Ratko, J.P. Cummings, J. Blebea, K.A. Matuszewski, Clinical gene therapy for nonmalignant disease, Am. J. Med. 115 (2003) 560–569. https://doi.org/10.1016/S0002-9343(03)00447-9.

[10]   D. Ibraheem, A. Elaissari, H. Fessi, Gene therapy and DNA delivery systems, Int. J. Pharm. 459 (2014) 70–83. https://doi.org/10.1016/J.IJPHARM.2013.11.041.

[11]   E. Hastie, R.J. Samulski, Adeno-Associated Virus at 50: A Golden Anniversary of Discovery, Research, and Gene Therapy Success - A Personal Perspective, Hum. Gene Ther. 26 (2015) 257–265. https://doi.org/10.1089/hum.2015.025.

[12]   J.A. Rose, M.D. Hoggan, A.J. Shatkin, Nucleic acid from an adeno-associated virus: chemical and physical studies., Proc. Natl. Acad. Sci. U. S. A. 56 (1966) 86–92. https://doi.org/10.1073/PNAS.56.1.86/ASSET/BBB21B12-DB63-4B59-AB57-07088960933B/ASSETS/PNAS.56.1.86.FP.PNG.

[13]   R.J. Samulski, N. Muzyczka, AAV-Mediated Gene Therapy for Research and Therapeutic Purposes, Https://Doi.Org/10.1146/Annurev-Virology-031413-085355 1 (2014) 427–451. https://doi.org/10.1146/ANNUREV-VIROLOGY-031413-085355.

[14]   T. Onishi, M. Nonaka, T. Maruno, Y. Yamaguchi, M. Fukuhara, T. Torisu, M. Maeda, S. Abbatiello, A. Haris, K. Richardson, K. Giles, S. Preece, N. Yamano-Adachi, T. Omasa, S. Uchiyama, Enhancement of recombinant adeno-associated virus activity by improved stoichiometry and homogeneity of capsid protein

assembly, Mol. Ther. Methods Clin. Dev. 31 (2023) 101142.

https://doi.org/10.1016/j.omtm.2023.101142.

[15] M. Naumer, F. Sonntag, K. Schmidt, K. Nieto, C. Panke, N.E. Davey, R. Popa-

Wagner, J.A. Kleinschmidt, Properties of the Adeno-Associated Virus Assembly-

Activating Protein, J. Virol. 86 (2012) 13038–13048.

https://doi.org/10.1128/JVI.01675-12/ASSET/26F16CCC-125B-412B-AAC4-

D3E7986C32ED/ASSETS/GRAPHIC/ZJV9990969070008.JPEG.

[16] L.F. Earley, J.M. Powers, K. Adachi, J.T. Baumgart, N.L. Meyer, Q. Xie, M.S.

Chapman, H. Nakai, Adeno-associated Virus (AAV) Assembly-Activating Protein

Is Not an Essential Requirement for Capsid Assembly of AAV Serotypes 4, 5, and

11, J. Virol. 91 (2017) 1980–1996. https://doi.org/10.1128/JVI.01980-

16/ASSET/9D61717C-1728-4DCE-805E-

17422558E7DF/ASSETS/GRAPHIC/ZJV9991822990010.JPEG.

[17] S. Daya, K.I. Berns, Gene therapy using adeno-associated virus vectors, Clin.

Microbiol. Rev. 21 (2008) 583–593. https://doi.org/10.1128/CMR.00008-08.

[18] V.W. Choi, D.M. McCarty, R.J. Samulski, Host Cell DNA Repair Pathways in

Adeno-Associated Viral Genome Processing, J. Virol. 80 (2006) 10346.

https://doi.org/10.1128/JVI.00841-06.

[19] S.A. Afione, C.K. Conrad, W.G. Kearns, S. Chunduru, R. Adams, T.C. Reynolds,

W.B. Guggino, G.R. Cutting, B.J. Carter, T.R. Flotte, In vivo model of adeno-

associated virus vector persistence and rescue., J. Virol. 70 (1996) 3235.

https://doi.org/10.1128/JVI.70.5.3235-3241.1996.

[20] M.F. Naso, B. Tomkowicz, W.L. Perry, W.R. Strohl, Adeno-Associated Virus (AAV) as a Vector for Gene Therapy, Biodrugs 31 (2017) 317. https://doi.org/10.1007/S40259-017-0234-5.

[21] T. Flotte, B. Carter, C. Conrad, W. Guggino, T. Reynolds, B. Rosenstein, G. Taylor, s. Walden, R. Wetzel, A Phase I Study of an Adeno-Associated Virus-CFTR Gene Vector in Adult CF Patients with Mild Lung Disease. Johns Hopkins Children's Center, Baltimore, Maryland, Https://Home.Liebertpub.Com/Hum 7 (2008) 1145–1159. https://doi.org/10.1089/HUM.1996.7.9-1145.

[22] P. Colella, G. Ronzitti, F. Mingozzi, Emerging Issues in AAV-Mediated In Vivo Gene Therapy, Mol. Ther. Methods Clin. Dev. 8 (2018) 87–104. https://doi.org/10.1016/J.OMTM.2017.11.007.

[23] C. Li, R.J. Samulski, Engineering adeno-associated virus vectors for gene therapy, Nat. Rev. Genet. 2020 214 21 (2020) 255–272. https://doi.org/10.1038/s41576-019-0205-4.

[24] M.W. Bolt, J.T. Brady, L.O. Whiteley, K.N. Khan, Development challenges associated with rAAV-based gene therapies, J. Toxicol. Sci. 46 (2021) 57–68. https://doi.org/10.2131/JTS.46.57.

[25] H.C. Verdera, K. Kuranda, F. Mingozzi, AAV Vector Immunogenicity in Humans: A Long Journey to Successful Gene Transfer, Mol. Ther. 28 (2020) 723–746. https://doi.org/10.1016/J.YMTHE.2019.12.010.

[26] J.A. Wagner, T. Reynolds, M.L. Moran, R.B. Moss, J.J. Wine, T.R. Flotte, P. Gardner, Efficient and persistent gene transfer of AAV-CFTR in maxillary sinus,

Lancet 351 (1998) 1702–1703. https://doi.org/10.1016/S0140-6736(05)77740-0.

[27] D. Wang, P.W.L. Tai, G. Gao, Adeno-associated virus vector as a platform for gene therapy delivery, Nat. Rev. Drug Discov. 2019 185 18 (2019) 358–378. https://doi.org/10.1038/s41573-019-0012-9.

[28] D.A. Kuzmin, M. V. Shutova, N.R. Johnston, O.P. Smith, V. V. Fedorin, Y.S. Kukushkin, J.C.M. van der Loo, E.C. Johnstone, The clinical landscape for AAV gene therapies, Nat. Rev. Drug Discov. 20 (2021) 173–174. https://doi.org/10.1038/D41573-021-00017-7.

[29] A.C. Nathwani, E.G.D. Tuddenham, S. Rangarajan, C. Rosales, J. McIntosh, D.C. Linch, P. Chowdary, A. Riddell, A.J. Pie, C. Harrington, J. O'Beirne, K. Smith, J. Pasi, B. Glader, P. Rustagi, C.Y.C. Ng, M.A. Kay, J. Zhou, Y. Spence, C.L. Morton, J. Allay, J. Coleman, S. Sleep, J.M. Cunningham, D. Srivastava, E. Basner-Tschakarjan, F. Mingozzi, K.A. High, J.T. Gray, U.M. Reiss, A.W. Nienhuis, A.M. Davidoff, Adenovirus-Associated Virus Vector–Mediated Gene Transfer in Hemophilia B, N. Engl. J. Med. 365 (2011) 2357–2365. https://www.nejm.org/doi/full/10.1056/NEJMoa1108046 (accessed February 4, 2021).

[30] R.E. MacLaren, M. Groppe, A.R. Barnard, C.L. Cottriall, T. Tolmachova, L. Seymour, K. Reed Clark, M.J. During, F.P.M. Cremers, G.C.M. Black, A.J. Lotery, S.M. Downes, A.R. Webster, M.C. Seabra, Retinal gene therapy in patients with choroideremia: Initial fi ndings from a phase 1/2 clinical trial, Lancet 383 (2014) 1129–1137. https://doi.org/10.1016/S0140-6736(13)62117-0.

[31]   L.M. Bryant, D.M. Christopher, A.R. Giles, C. Hinderer, J.L. Rodriguez, J.B.
       Smith, E.A. Traxler, J. Tycko, A.P. Wojno, J.M. Wilson, Lessons Learned from the
       Clinical Development and Market Authorization of Glybera,
       Https://Home.Liebertpub.Com/Humc 24 (2013) 55–64.
       https://doi.org/10.1089/HUMC.2013.087.

[32]   A.C. Nathwani, U.M. Reiss, E.G.D. Tuddenham, C. Rosales, P. Chowdary, J.
       McIntosh, M. Della Peruta, E. Lheriteau, N. Patel, D. Raj, A. Riddell, J. Pie, S.
       Rangarajan, D. Bevan, M. Recht, Y.-M. Shen, K.G. Halka, E. Basner-
       Tschakarjan, F. Mingozzi, K.A. High, J. Allay, M.A. Kay, C.Y.C. Ng, J. Zhou, M.
       Cancio, C.L. Morton, J.T. Gray, D. Srivastava, A.W. Nienhuis, A.M. Davidoff,
       Long-Term Safety and Efficacy of Factor IX Gene Therapy in Hemophilia B, N.
       Engl. J. Med. 371 (2014) 1994–2004.
       https://doi.org/10.1056/NEJMOA1407309/SUPPL_FILE/NEJMOA1407309_DISC
       LOSURES.PDF.

[33]   List of Approved Regenerative Medical Products, (2015).
       https://www.pmda.go.jp/english/review-services/reviews/approved-
       information/0004.html (accessed January 31, 2024).

[34]   K. Crowe, The million-dollar drug | CBC News, CBC News (2018).
       https://newsinteractives.cbc.ca/longform/glybera (accessed November 2, 2021).

[35]   A. Keowon, Top 10 Most Expensive Drugs on the Market, Biospace (2021).
       https://www.biospace.com/article/gene-therapy-zolgensma-tops-goodrx-list-of-10-
       most-expensive-drugs/ (accessed November 2, 2021).

[36]   FDA approves most expensive drug ever, a $3.5 million-per-dose gene therapy for hemophilia B - CBS News, (n.d.). https://www.cbsnews.com/news/fda-approves-hemgenix-most-expensive-drug-hemophilia-b/ (accessed April 15, 2024).

[37]   N. Clément, J.C. Grieger, Manufacturing of recombinant adeno-associated viral vectors for clinical trials, Nature Publishing Group, 2016. https://doi.org/10.1038/mtm.2016.2.

[38]   M.S. Goodwin, C.L. Croft, H.S. Futch, D. Ryu, C. Ceballos-Diaz, X. Liu, G. Paterno, C. Mejia, D. Deng, K. Menezes, L. Londono, K. Arjona, M. Parianos, V. Truong, E. Rostonics, A. Hernandez, S.L.S.E. Boye, S.L.S.E. Boye, Y. Levites, P.E. Cruz, T.E. Golde, Utilizing minimally purified secreted rAAV for rapid and cost-effective manipulation of gene expression in the CNS, Mol. Neurodegener. 15 (2020) 1–16. https://doi.org/10.1186/s13024-020-00361-z.

[39]   E. Ayuso, F. Mingozzi, F. Bosch, Production, Purification and Characterization of Adeno-Associated Vectors, Curr. Gene Ther. 10 (2010) 423–436. https://doi.org/10.2174/156652310793797685.

[40]   A. Srivastava, K.M.G. Mallela, N. Deorkar, G. Brophy, Manufacturing Challenges and Rational Formulation Development for AAV Viral Vectors, J. Pharm. Sci. 110 (2021) 2609–2624. https://doi.org/10.1016/j.xphs.2021.03.024.

[41]   J.F. Wright, T. Le, J. Prado, J. Bahr-Davidson, P.H. Smith, Z. Zhen, J.M. Sommer, G.F. Pierce, G. Qu, Identification of factors that contribute to recombinant AAV2 particle aggregation and methods to prevent its occurrence during vector

purification and formulation, Mol. Ther. 12 (2005) 171–178.

[42] J.F. Wright, Product-Related Impurities in Clinical-Grade Recombinant AAV Vectors: Characterization and Risk Assessment, Biomed. 2014, Vol. 2, Pages 80-97 2 (2014) 80–97. https://doi.org/10.3390/BIOMEDICINES2010080.

[43] H. Nygren, M. Stenbergt, Immunochemistry at interfaces., Immunology 66 (1989) 321. /pmc/articles/PMC1385214/?report=abstract (accessed February 2, 2024).

[44] W. Wang, S. Nema, D. Teagarden, Protein aggregation—Pathways and influencing factors, Int. J. Pharm. 390 (2010) 89–99. https://doi.org/10.1016/J.IJPHARM.2010.02.025.

[45] W. Wang, S. Singh, D.L. Zeng, K. King, S. Nema, Antibody Structure, Instability, and Formulation, J. Pharm. Sci. 96 (2007) 1–26. https://doi.org/10.1002/JPS.20727.

[46] W. Wang, Protein aggregation and its inhibition in biopharmaceutics, Int. J. Pharm. 289 (2005) 1–30. https://doi.org/10.1016/J.IJPHARM.2004.11.014.

[47] E. Sun, J. He, X. Zhuang, Live cell imaging of viral entry, Curr. Opin. Virol. 3 (2013) 34–43. https://doi.org/10.1016/J.COVIRO.2013.01.005.

[48] D. Mudhakir, H. Harashima, Learning from the viral journey: How to enter cells and how to overcome intracellular barriers to reach the nucleus, AAPS J. 11 (2009) 65–77. https://doi.org/10.1208/S12248-009-9080-9/FIGURES/3.

[49] D. Liu, L. Pan, H. Zhai, H.J. Qiu, Y. Sun, Virus tracking technologies and their applications in viral life cycle: research advances and future perspectives, Front.

Immunol. 14 (2023). https://doi.org/10.3389/FIMMU.2023.1204730.

[50] J.F. Wright, G. Qu, C. Tang, J.M. Sommer, Recombinant adeno-associated virus:
      formulation challenges and strategies for a gene therapy vector., Curr. Opin.
      Drug Discov. Devel. 6 (2003) 174–178.
      https://europepmc.org/article/med/12669452 (accessed December 29, 2023).

[51] J. Bennicelli, J.F. Wright, A. Komaromy, J.B. Jacobs, B. Hauck, O. Zelenaia, F.
      Mingozzi, D. Hui, D. Chung, T.S. Rex, Z. Wei, G. Qu, S. Zhou, C. Zeiss, V.R.
      Arruda, G.M. Acland, L.F. Dell'Osso, K.A. High, A.M. Maguire, J. Bennett,
      Reversal of blindness in animal models of leber congenital amaurosis using
      optimized AAV2-mediated gene transfer, Mol. Ther. 16 (2008) 458–465.
      https://doi.org/10.1038/sj.mt.6300389.

[52] C.A. Reid, D.M. Lipinski, Small and micro-scale recombinant adeno-associated
      virus production and purification for ocular gene therapy applications, Methods
      Mol. Biol. 1715 (2018) 19–31. https://doi.org/10.1007/978-1-4939-7522-8_2.

[53] M. Jiang, C.M. Dupuis, A.A. Medeiros, S.C. Wadsworth, K.R. Clark, C.J.
      Morrison, 710. Surface Adsorptive Loss of rAAV on Materials Used in cGMP
      Manufacturing, Mol. Ther. 24 (2016) S280. https://doi.org/10.1016/s1525-
      0016(16)33518-3.

[54] Y. Zhang, T. Ogura, J. Mimuro, T. Okada, A. Kume, Y. Sakata, K. Ozawa, H.
      Mizukami, L. Perabo, J. Endell, S. King, D. Goldnau, K. Lux, M. Hallek, H.
      Buening, 864. Adsorption of Adeno-Associated Virus to Commonly Used Catheter
      Materials, Mol. Ther. 11 (2005) S335.

https://doi.org/10.1016/j.ymthe.2005.07.407.

[55] D.P. Cross, M. Morris, 512. Characterization of Adsorption of Adeno-Associated Virus to Commonly Used Catheter Materials: AAV2 vs. AAV1/2, Mol. Ther. 13 (2006) S197. https://doi.org/10.1016/j.ymthe.2006.08.582.

[56] E. Bunting, S, Colosi, PC and Pungor, Adeno-associated virus factor Viii vectors, associated viral particles, and therapeutic formulations comprising the same, 2012. https://patents.google.com/patent/WO2017053677A1/en (accessed September 7, 2021).

[57] C. Kraft, K.E. Glen, J. Harriman, R. Thomas, A.M. Lyness, Evaluation of a novel cyclic olefin polymer container system for cryopreservation of adeno-associated virus, Cytotherapy 22 (2020) S147–S148. https://doi.org/10.1016/J.JCYT.2020.03.300.

[58] M.P. Starkey, R. Elaswarapu, T.J. Amiss, R.J. Samulski, Methods for Adeno-Associated Virus-Mediated Gene Transfer into Muscle, Methods Mol. Biol. 175 (2001) 455–469. https://doi.org/10.1385/1-59259-235-X:455.

[59] M. Lock, S. McGorray, A. Auricchio, E. Ayuso, E.J. Beecham, V. Blouin-Tavel, F. Bosch, M. Bose, B.J. Byrne, T. Caton, J.A. Chiorini, A. Chtarto, K.R. Clark, T. Conlon, C. Darmon, M. Doria, A. Douar, T.R. Flotte, J.D. Francis, A. Francois, M. Giacca, M.T. Korn, I. Korytov, X. Leon, B. Leuchs, G. Lux, C. Melas, H. Mizukami, P. Moullier, M. Müller, K. Ozawa, T. Philipsberg, K. Poulard, C. Raupp, C. Rivière, S.D. Roosendaal, R.J. Samulski, S.M. Soltys, R. Surosky, L. Tenenbaum, D.L. Thomas, B. Van Montfort, G. Veres, J.F. Wright, Y. Xu, O. Zelenaia, L. Zentilin,

R.O. Snyder, Characterization of a recombinant adeno-associated virus type 2 reference standard material, Hum. Gene Ther. 21 (2010) 1273–1285. https://doi.org/10.1089/hum.2009.223.

[60] L.M. Sanftner, J.M. Sommer, B.M. Suzuki, P.H. Smith, S. Vijay, J.A. Vargas, J.R. Forsayeth, J. Cunningham, K.S. Bankiewicz, H. Kao, J. Bernal, G.F. Pierce, K.W. Johnson, AAV2-mediated gene delivery to monkey putamen: Evaluation of an infusion device and delivery parameters, Exp. Neurol. 194 (2005) 476–483. https://doi.org/10.1016/j.expneurol.2005.03.007.

[61] 525. Evaluation of Formulation and Stability of Investigational Gene Transfer Vectors for Leber Congenital Amaurosis, Mol. Ther. 15 (2007) S202. https://doi.org/10.1016/S1525-0016(16)44731-3.

[62] K.S. Bankiewicz, J.L. Eberling, M. Kohutnicka, W. Jagust, P. Pivirotto, J. Bringas, J. Cunningham, T.F. Budinger, J. Harvey-White, Convection-Enhanced Delivery of AAV Vector in Parkinsonian Monkeys; In Vivo Detection of Gene Expression and Restoration of Dopaminergic Function Using Pro-drug Approach, Exp. Neurol. 164 (2000) 2–14. https://doi.org/10.1006/EXNR.2000.7408.

[63] M.I. Patrício, C.I. Cox, C. Blue, A.R. Barnard, C. Martinez-Fernandez de la Camara, R.E. MacLaren, Inclusion of PF68 Surfactant Improves Stability of rAAV Titer when Passed through a Surgical Device Used in Retinal Gene Therapy, Mol. Ther. - Methods Clin. Dev. 17 (2020) 99–106. https://doi.org/10.1016/j.omtm.2019.11.005.

[64] J.M. Escandell, D.A. Pais, S.B. Carvalho, K. Vincent, P. Gomes-Alves, P.M.

Alves, Leveraging rAAV bioprocess understanding and next generation

bioanalytics development, Curr. Opin. Biotechnol. 74 (2022) 271–277.

https://doi.org/10.1016/J.COPBIO.2021.12.009.

[65] J.S. Katz, D.K. Chou, T.R. Christian, T.K. Das, M. Patel, S.N. Singh, Y. Wen,

Emerging Challenges and Innovations in Surfactant-mediated Stabilization of

Biologic Formulations, J. Pharm. Sci. 111 (2022) 919–932.

https://doi.org/10.1016/J.XPHS.2021.12.002.

[66] J.G. Moloughney, N. Weisleder, Poloxamer 188 (P188) as a Membrane

Resealing Reagent in Biomedical Applications, Recent Pat. Biotechnol. 6 (2012)

200. https://doi.org/10.2174/1872208311206030200.

[67] W.N. Chen, M.F. Shaikh, S. Bhuvanendran, A. Date, M.T. Ansari, A.K.

Radhakrishnan, I. Othman, Poloxamer 188 (P188), A Potential Polymeric

Protective Agent for Central Nervous System Disorders: A Systematic Review,

Curr. Neuropharmacol. 20 (2022) 799.

https://doi.org/10.2174/1570159X19666210528155801.

[68] R. Rieser, M. Penaud-Budloo, M. Bouzelha, A. Rossi, T. Menzen, M. Biel, H.

Büning, E. Ayuso, G. Winter, S. Michalakis, Intrinsic Differential Scanning

Fluorimetry for Fast and Easy Identification of Adeno-Associated Virus Serotypes,

J. Pharm. Sci. 109 (2020) 854–862. https://doi.org/10.1016/j.xphs.2019.10.031.

[69] FDA, Inactive Ingredient Search for Approved Drug Products, U.S Food Drug

Adm. 20993 (2020).

https://www.accessdata.fda.gov/scripts/cder/iig/index.Cfm?event=BasicSearch.pa

ge (accessed November 2, 2021).

[70] P.M. Quinn, T.M. Buck, C. Ohonin, H.M.M. Mikkers, J. Wijnholds, Production of iPS-derived human retinal organoids for use in transgene expression assays, in: Methods Mol. Biol., Humana Press Inc., 2018: pp. 261–273. https://doi.org/10.1007/978-1-4939-7522-8_19.

[71] M.D. Fischer, D.G. Hickey, M.S. Singh, R.E. MacLaren, Evaluation of an Optimized Injection System for Retinal Gene Therapy in Human Patients, Hum. Gene Ther. Methods 27 (2016) 150–158. https://doi.org/10.1089/hgtb.2016.086.

[72] W.A. Beltran, A. V. Cideciyan, A.S. Lewin, S. Iwabe, H. Khanna, A. Sumaroka, V.A. Chiodo, D.S. Fajardo, A.J. Román, W.T. Deng, M. Swider, T.S. Alemán, S.L. Boye, S. Genini, A. Swaroop, W.W. Hauswirth, S.G. Jacobson, G.D. Aguirre, Gene therapy rescues photoreceptor blindness in dogs and paves the way for treating human X-linked retinitis pigmentosa, Proc. Natl. Acad. Sci. U. S. A. 109 (2012) 2132–2137. https://doi.org/10.1073/pnas.1118847109.

[73] S. Nema, R.J. Washkuhn, R.J. Brendel, Excipients and Their Use in Injectable Products, PDA J. Pharm. Sci. Technol. 51 (1997).

[74] E.V. Brovč, J. Mravljak, R. Šink, S. Pajk, Rational design to biologics development: The polysorbates point of view, Int. J. Pharm. 581 (2020) 119285. https://doi.org/10.1016/J.IJPHARM.2020.119285.

[75] Fda, Package Insert - HEMGENIX, (n.d.). www.fda.gov/medwatch. (accessed January 31, 2024).

[76] F.C. Hewitt, C. Li, S.J. Gray, S. Cockrell, M. Washburn, R.J. Samulski, Reducing the Risk of Adeno-Associated Virus (AAV) Vector Mobilization with AAV Type 5 Vectors, J. Virol. 83 (2009) 3919–3929. https://doi.org/10.1128/jvi.02466-08.

[77] S. Hagen, T. Baumann, H.J. Wagner, V. Morath, B. Kaufmann, A. Fischer, S. Bergmann, P. Schindler, K.M. Arndt, K.M. Müller, Modular adeno-associated virus (rAAV) vectors used for cellular virus-directed enzyme prodrug therapy, Sci. Rep. 4 (2014) 1–11. https://doi.org/10.1038/srep03759.

[78] C. Aurnhammer, M. Haase, N. Muether, M. Hausl, C. Rauschhuber, I. Huber, H. Nitschko, U. Busch, A. Sing, A. Ehrhardt, A. Baiker, Universal real-time PCR for the detection and quantification of adeno-associated virus serotype 2-derived inverted terminal repeat sequences, Hum. Gene Ther. Methods 23 (2012) 18–28. https://doi.org/10.1089/hgtb.2011.034.

[79] I. Spark Therapeutics, Highlights of Prescribing Information, 2017. https://www.fda.gov/media/109906/download (accessed November 1, 2021).

[80] S.K. Singh, H.C. Mahler, C. Hartman, C.A. Stark, Are Injection Site Reactions in Monoclonal Antibody Therapies Caused by Polysorbate Excipient Degradants?, J. Pharm. Sci. 107 (2018) 2735–2741. https://doi.org/10.1016/J.XPHS.2018.07.016.

[81] Pluronic® F-68 solid, BioReagent, suitable for cell culture, suitable for insect cell culture | 9003-11-6, (n.d.). https://www.sigmaaldrich.com/JP/en/product/SIGMA/P1300 (accessed November 1, 2021).

[82] Kolliphor® P 188 | 9003-11-6, (n.d.).

https://www.sigmaaldrich.com/JP/en/product/sigma/15759 (accessed November 1, 2021).

[83] W. Chen, S. Stolz, V. Wegbecher, D. Parakkattel, C. Haeuser, N.S. Oltra, R.S.K. Kishore, S. Bond, C. Bell, R. Kopf, The degradation of poloxamer 188 in buffered formulation conditions, AAPS Open 2022 81 8 (2022) 1–13. https://doi.org/10.1186/S41120-022-00055-4.

[84] M.T. Jones, H.C. Mahler, S. Yadav, D. Bindra, V. Corvari, R.M. Fesinmeyer, K. Gupta, A.M. Harmon, K.D. Hinds, A. Koulov, W. Liu, K. Maloney, J. Wang, P.Y. Yeh, S.K. Singh, Considerations for the Use of Polysorbates in Biopharmaceuticals, Pharm. Res. 35 (2018) 1–8. https://doi.org/10.1007/S11095-018-2430-5/FIGURES/2.

[85] M.A. Croyle, X. Cheng, J.M. Wilson, Development of formulations that enhance physical stability of viral vectors for gene therapy, Gene Ther. 8 (2001) 1281–1290. https://doi.org/10.1038/sj.gt.3301527.

[86] H. Elwing, S. Welin, A. Askendal, U. Nilsson, I. LundstrÖm, A wettability gradient method for studies of macromolecular interactions at the liquid/solid interface, J. Colloid Interface Sci. 119 (1987) 203–210. https://doi.org/10.1016/0021-9797(87)90260-8.

[87] S. Welin-Klintström, A. Askendal, H. Elwing, Surfactant and protein interactions on wettability gradient surfaces, J. Colloid Interface Sci. 158 (1993) 188–194. https://doi.org/10.1006/jcis.1993.1246.

[88] Nissan Chemical Corporation/Planning and Development Division, (n.d.).

https://www.nissanchem.co.jp/eng/products/advance/prevelex.html (accessed February 5, 2021).

[89]   H. Tateno, K. Hiemori, F. Minoshima, K. Kiyoi, K. Matoba, J. Katayama, Y. Kumada, Oriented immobilization of rBC2LCN lectin for highly sensitive detection of human pluripotent stem cells using cell culture supernatants, J. Biosci. Bioeng. 129 (2020) 215–222. https://doi.org/10.1016/J.JBIOSC.2019.08.003.

[90]   Y. Wang, N. Menon, S. Shen, M. Feschenko, S. Bergelson, A qPCR Method for AAV Genome Titer with ddPCR-Level of Accuracy and Precision, Mol. Ther. Methods Clin. Dev. 19 (2020) 341–346. https://doi.org/10.1016/j.omtm.2020.09.017.

[91]   D. Dobnik, P. Kogovšek, T. Jakomin, N. Košir, M. Tušek Žnidarič, M. Leskovec, S.M. Kaminsky, J. Mostrom, H. Lee, M. Ravnikar, M.T. Žnidarič, M. Leskovec, S.M. Kaminsky, J. Mostrom, H. Lee, M. Ravnikar, Accurate Quantification and Characterization of Adeno-Associated Viral Vectors, Front. Microbiol. 0 (2019) 1570. https://doi.org/10.3389/FMICB.2019.01570.

[92]   T.M.G. Selva, J.S.G. Selva, R.B. Prata, Sensing Materials: Diamond-Based Materials, Encycl. Sensors Biosens. Vol. 1-4, First Ed. 1–4 (2023) 45–72. https://doi.org/10.1016/B978-0-12-822548-6.00081-9.

[93]   7 ways to measure contact angle, (n.d.). https://www.biolinscientific.com/blog/7-ways-to-measure-contact-angle (accessed February 13, 2024).

[94]   A review of contact angle techniques | Contact Lens Update, (n.d.). https://contactlensupdate.com/2017/01/31/a-review-of-contact-angle-techniques/

(accessed February 13, 2024).

[95] Zeta potential | Anton Paar Wiki, (n.d.). https://wiki.anton-paar.com/en/zeta-potential/ (accessed February 13, 2024).

[96] Zeta Potential (ZP): An Overview and ZP Guide | LLS Health CDMO, (n.d.). https://lubrizolcdmo.com/technical-briefs/overview-of-the-zeta-potential/ (accessed February 13, 2024).

[97] Zeta Potential - Brookhaven Instruments, (n.d.). https://www.brookhaveninstruments.com/particle-characterization-applications/zeta-potential/ (accessed February 15, 2024).

[98] L.C. Xu, C.A. Siedlecki, Effects of surface wettability and contact time on protein adhesion to biomaterial surfaces, Biomaterials 28 (2007) 3273–3283. https://doi.org/10.1016/j.biomaterials.2007.03.032.

[99] H. Kitano, K. Nagaoka, S. Tada, M. Gemmei-Ide, M. Tanaka, Structure of water incorporated in amphoteric polymer thin films as revealed by FT-IR spectroscopy, Macromol. Biosci. 8 (2008) 77–85. https://doi.org/10.1002/mabi.200700082.

[100] T. Goda, R. Matsuno, T. Konno, M. Takai, K. Ishihara, Protein adsorption resistance and oxygen permeability of chemically crosslinked phospholipid polymer hydrogel for ophtnalmologie biomaterials, J. Biomed. Mater. Res. - Part B Appl. Biomater. 89 (2009) 184–190. https://doi.org/10.1002/jbm.b.31204.

[101] O. H, O. H, I. P, I. P, I. Novartis Gene Therapies, Highlights of prescribing information, 2008.

https://www.novartis.us/sites/www.novartis.us/files/zolgensma.pdf (accessed November 1, 2021).

[102] Addgene, Addgene: AAV Titration by qPCR, (n.d.). https://www.addgene.org/protocols/aav-titration-qpcr-using-sybr-green-technology/ (accessed November 1, 2021).

[103] A.S. Van Dyke, D. Collard, M.M. Derby, A.R. Betz, Droplet coalescence and freezing on hydrophilic, hydrophobic, and biphilic surfaces, Appl. Phys. Lett. 107 (2015) 141602. https://doi.org/10.1063/1.4932050.

[104] J. Sanmiguel, G. Gao, L.H. Vandenberghe, Quantitative and digital droplet-based AAV genome titration, in: Methods Mol. Biol., Humana Press Inc., 2019: pp. 51–83. https://doi.org/10.1007/978-1-4939-9139-6_4.

[105] Captive bubble measurements - Nanoscience Instruments, (n.d.). https://www.nanoscience.com/techniques/tensiometry/captive-bubble-measurements/ (accessed November 1, 2021).

[106] D. Campbell, S.M. Carnell, R.J. Eden, Applicability of contact angle techniques used in the analysis of contact lenses, part 1: comparative methodologies., Eye Contact Lens 39 (2013) 254–62. https://doi.org/10.1097/ICL.0b013e31828ca174.

[107] W. Wang, Instability, stabilization, and formulation of liquid protein pharmaceuticals, Int. J. Pharm. 185 (1999) 129–188. https://doi.org/10.1016/S0378-5173(99)00152-0.

[108] L. Meagher, R.M. Pashley, Interaction Forces between Silica and Polypropylene

Surfaces in Aqueous Solution, Langmuir 11 (1995) 4019–4024.

https://pubs.acs.org/sharingguidelines (accessed January 18, 2024).

[109] G. Atun, G. Hisarli, M. Tunçay, Adsorption of safranine-O on hydrophilic and hydrophobic glass surfaces, Colloids Surfaces A Physicochem. Eng. Asp. 143 (1998) 27–33. https://doi.org/10.1016/S0927-7757(98)00494-4.

[110] B.A. Jucker, H. Harms, A.J.B. Zehnder, Adhesion of the positively charged bacterium Stenotrophomonas (Xanthomonas) maltophilia 70401 to glass and teflon, J. Bacteriol. 178 (1996) 5472–5479. https://doi.org/10.1128/JB.178.18.5472-5479.1996.

[111] T.F. Broekhoff, C.C.G. Sweegers, E.M. Krijkamp, A.K. Mantel-Teeuwisse, H.G.M. Leufkens, W.G. Goettsch, R.A. Vreman, Early Cost-Effectiveness of Onasemnogene Abeparvovec-xioi (Zolgensma) and Nusinersen (Spinraza) Treatment for Spinal Muscular Atrophy I in The Netherlands With Relapse Scenarios, Value Heal. 24 (2021) 759–769. https://doi.org/10.1016/J.JVAL.2020.09.021.

[112] G. Gomori, [16] Preparation of buffers for use in enzyme studies, Methods Enzymol. 1 (1955) 138–146. https://doi.org/10.1016/0076-6879(55)01020-3.

[113] A. Bennett, S. Patel, M. Mietzsch, A. Jose, B. Lins-Austin, J.C. Yu, B. Bothner, R. McKenna, M. Agbandje-McKenna, Thermal Stability as a Determinant of AAV Serotype Identity, Mol. Ther. - Methods Clin. Dev. 6 (2017) 171–182. https://doi.org/10.1016/j.omtm.2017.07.003.

[114] F. Ramírez, J. Wu, C. Haitjema, C. Heger, Development of a highly sensitive

imaged cIEF immunoassay for studying AAV capsid protein charge heterogeneity, Electrophoresis 44 (2023) 1258–1266. https://doi.org/10.1002/ELPS.202300039.

[115] T. Elich, T. Cheung, K. Calnan, Chromatography Solutions for AAV Full and Empty Capsid Separation, (n.d.).

[116] O.-W. Merten, M. Al-Rubeai, eds., Viral Vectors for Gene Therapy, Humana Press, Totowa, NJ, 2011. https://doi.org/10.1007/978-1-61779-095-9.

[117] Recombinant Adeno-associated virus 2 | ATCC, (n.d.). https://www.atcc.org/products/vr-1616 (accessed November 2, 2021).

[118] A.C.N. Vr-, W.G. Aavrswg, Product Information Sheet for ATCC □ VR-1616 ᵀᴹ COLLECTION OF ANIMAL VIRUSES , CHLAMYDIAE and RICKETTSIAE Reference Standard Stock (rAAV2-RSS) COLLECTION OF ANIMAL VIRUSES , CHLAMYDIAE and RICKETTSIAE, n.d. https://www.atcc.org/-/media/product-assets/documents/protocols/virology/vr-1616.pdf?rev=097cd3d9bbab408da2a6b4d1315bb80f.

[119] E. Ayuso, V. Blouin, M. Lock, S. Mcgorray, X. Leon, M.R. Alvira, A. Auricchio, S. Bucher, A. Chtarto, K.R. Clark, C. Darmon, M. Doria, W. Fountain, G. Gao, K. Gao, M. Giacca, J. Kleinschmidt, B. Leuchs, C. Melas, H. Mizukami, M. Müller, Y. Noordman, O. Bockstael, K. Ozawa, C. Pythoud, M. Sumaroka, R. Surosky, L. Tenenbaum, I. Van Der Linden, B. Weins, J.F. Wright, X. Zhang, L. Zentilin, F. Bosch, R.O. Snyder, P. Moullier, Manufacturing and characterization of a recombinant adeno-associated virus type 8 reference standard material, Hum. Gene Ther. 25 (2014) 977–987. https://doi.org/10.1089/hum.2014.057.

[120] S.C. Taylor, K. Nadeau, M. Abbasi, C. Lachance, M. Nguyen, J. Fenrich, The Ultimate qPCR Experiment: Producing Publication Quality, Reproducible Data the First Time, Trends Biotechnol. 37 (2019) 761–774. https://doi.org/10.1016/J.TIBTECH.2018.12.002.

[121] S. Branford, L. Fletcher, N.C.P. Cross, M.C. Müller, A. Hochhaus, D.-W. Kim, J.P. Radich, G. Saglio, F. Pane, S. Kamel-Reid, Y.L. Wang, R.D. Press, K. Lynch, Z. Rudzki, J.M. Goldman, T. Hughes, Desirable performance characteristics for BCR-ABL measurement on an international reporting scale to allow consistent interpretation of individual patient response and comparison of response rates between clinical trials, Blood 112 (2008) 3330–3338. https://doi.org/10.1182/BLOOD-2008-04-150680.

[122] K.J. Albert, J.T. Bradshaw, Importance of Integrating a Volume Verification Method for Liquid Handlers: Applications in Learning Performance Behavior, JALA J. Assoc. Lab. Autom. 12 (2007) 172–180. https://doi.org/10.1016/j.jala.2006.10.005.

[123] S. Pacouret, M. Bouzelha, R. Shelke, E. Andres-Mateos, R. Xiao, A. Maurer, M. Mevel, H. Turunen, T. Barungi, M. Penaud-Budloo, F. Broucque, V. Blouin, P. Moullier, E. Ayuso, L.H. Vandenberghe, AAV-ID: A Rapid and Robust Assay for Batch-to-Batch Consistency Evaluation of AAV Preparations, Mol. Ther. 25 (2017) 1375–1386. https://doi.org/10.1016/J.YMTHE.2017.04.001.